NASA TECHNICAL MEMORANDUM

UB
NASA TM X-1347

LOW-SPEED WIND-TUNNEL TESTS OF A FULL-SCALE M2-F2 LIFTING BODY MODEL

by Kenneth W. Mort and Berl Gamse

Ames Research Center
Moffett Field, Calif.

NATIONAL AERONAUTICS AND SPACE ADMINISTRATION • WASHINGTON, D. C. • FEBRUARY 1967

NASA TM X-1347

LOW-SPEED WIND-TUNNEL TESTS OF A FULL-SCALE M2-F2 LIFTING BODY MODEL

By Kenneth W. Mort and Berl Gamse

Ames Research Center
Moffett Field, Calif.

NATIONAL AERONAUTICS AND SPACE ADMINISTRATION

[redacted]

LOW-SPEED WIND-TUNNEL TESTS OF A FULL-SCALE M2-F2 LIFTING BODY MODEL*

By Kenneth W. Mort and Berl Gamse
Ames Research Center

SUMMARY

The longitudinal and lateral-directional aerodynamic characteristics of the M2-F2 lifting body model were investigated in the Ames 40- by 80-Foot Wind Tunnel. The M2-F2 configuration was based on the M2-F1 design with modifications to the afterbody, the control surfaces, and the canopy location. The effects of modifications to the model during the test series, but not incorporated in the final M2-F2 configuration, are also included.

The investigation was conducted over a range of angles of attack from -8° to $+28^\circ$, angles of sideslip from -5° to $+10^\circ$, and free-stream dynamic pressures from 17 to 97 lb/ft^2. The results indicated that the M2-F2 configuration was longitudinally stable over the entire trimmed lift-coefficient range investigated, from 0 to 0.9. There was no evidence of stall except at the extreme combination of 24° angle of attack and 10° angle of sideslip. The maximum lift-to-drag ratios realized for the M2-F2 configuration were 4.2 untrimmed and 4.0 trimmed.

INTRODUCTION

Studies of lifting body reentry vehicles capable of controlled gliding flight and conventional horizontal landings resulted in the basic M2-F1 design (see refs. 1-7). The results of wind-tunnel and flight tests of this vehicle configuration are reported in reference 8, 9, and 10. The design of the control surfaces, the afterbody, and the canopy was modified to improve the low-speed performance and handling characteristics of the vehicle and to make the configuration compatible with high-speed flight requirements. This modified configuration was designated the M2-F2. The low-speed aerodynamic characteristics determined by full-scale wind-tunnel tests of this modified design and the effects of other modifications tested during the investigations leading to the definition of the M2-F2 configuration are reported here.

NOTATION

b maximum span, 9.51 ft

C_D drag coefficient, $\frac{D}{qS}$

*Title, Unclassified

[redacted]

C_L lift coefficient, $\frac{L}{qS}$

C_l rolling-moment coefficient, $\frac{\text{rolling moment}}{qSb}$

C_m pitching-moment coefficient, $\frac{\text{pitching moment}}{qSl}$

C_n yawing-moment coefficient, $\frac{\text{yawing moment}}{qSb}$

C_Y side-force coefficient, $\frac{\text{side force}}{qS}$

D drag force, lb

L lift force, lb

l reference length (original length of M2), 20 ft

q free-stream dynamic pressure, lb/ft^2

R_n Reynolds number, $\frac{\text{free-stream velocity}}{\text{kinematic viscosity}} \times l$

S reference area (original body planform area of M2), 138.9 ft^2

α angle of attack, angle between cone axis and free stream, deg

β angle of sideslip, deg

δ_a differential upper flap or elevon deflection, deg left roll is (+) δ_a

δ_l lower flap deflection, deg

δ_r rudder deflection, deg

δ_u upper flap deflection, deg

Superscript

r radius, in.

The forces developed by the model were resolved along the wind axes and the moments about the body axes.

The sign convention for control surface deflections, forces, and angles is given in figure 1. Zero angle on all control surfaces is defined as that position where the control surface is tangent with the model surface immediately upstream of the control hinge line.

MODEL DESCRIPTION

The model is shown in figure 2 installed in the 40- by 80-foot wind tunnel. The model dimensions are presented in figure 3. The body of the model forward of station 240 was made from a fiber glass mold of a plywood construction flight vehicle (M2-F1). Deviations of that flight vehicle's dimensions from those in figure 3 were repeated on the model. The model construction, therefore, is typical of large-scale wind-tunnel models in regard to air leakage, control surface attachments, and rigidity but is not typical in regard to dimensional tolerances and surface conditions.

The control system of the M2-F2 configuration (figs. 1 and 3(a)) included upper-surface flaps that moved together for longitudinal control and differentially for lateral control, and lower-surface flaps that could be used independently or in conjunction with the upper flaps for longitudinal control. The lower-surface flaps were limited to a minimum deflection of 10° and were always deflected together. The model had split flap-type rudders on the outboard surfaces of the vertical stabilizer with only one surface deflecting outboard at a time for directional control.

The devices investigated included (figs. 3(b), 3(c), and 3(d)) the boattail fairing (which was incorporated into the final M2-F2 configuration) elevons at the base of the vertical stabilizer, flaps with their hinge line at the trailing edge of the afterbody, quasi-wings simulating landing gear doors, outboard ventral fins, and a central dorsal fin.

TESTING PROCEDURE

The aerodynamic characteristics were obtained by varying the angle of attack from -12° to +28° for several control settings and for sideslip angles of -5°, 0°, +5°, and +10°. The effects of Reynolds number were investigated at one longitudinal control setting and zero sideslip for Reynolds numbers from 20×10^6 to 36×10^6. Unless otherwise noted on the figures, the investigation was performed at a Reynolds number of 36×10^6 (dynamic pressure of 97 lb/ft^2).

DATA REDUCTION

Accuracy of Data

The accuracy of the data presented, estimated from possible errors in measurements, instrumentation, and recording, is as follows:

Lift	±10 lb	Rolling moment	±400 ft-lb
Drag	±3 lb	Dynamic pressure	±0.5 percent
Side force	±3 lb	Angle of attack	±0.2°
Pitching moment	±300 ft-lb	Control surface deflection	±0.5°
Yawing moment	±100 ft-lb		

Corrections to the Data

The data were corrected to account for the unshielded main strut tips and tail strut and for the fairing between the main strut tip and the body (fig. 2).

The strut tip and tail strut tare values used were:

$$C_D = 0.052 - 0.020 \sin \alpha$$

$$C_m = -0.031 + 0.001 \sin \alpha$$

$$C_n = 0.0518 \sin \beta$$

$$C_l = 0.0082 - 0.0116 \sin \alpha$$

The fairing tare values used were:

$$C_L = 0.111 \sin \alpha , \quad \alpha \leq 18^\circ$$

$$= 0.034 - 0.093 \sin(\alpha - 18^\circ) , \quad \alpha > 18^\circ$$

$$C_D = 0.389 - 0.389 \cos \alpha - 0.020 \sin \alpha , \quad \alpha \leq 16^\circ$$

$$= 0.01 , \quad \alpha > 16^\circ$$

$$C_m = -0.262 + 0.262 \cos \alpha + 0.0124 \sin \alpha , \quad \alpha \leq 16^\circ$$

$$= -0.007 + 0.055 \sin(\alpha - 16^\circ) , \quad \alpha > 16^\circ$$

RESULTS AND DISCUSSION

The results are presented in two parts, the first part documents the aerodynamic characteristics of the M2-F2 configuration, and the second presents the effects of the various devices investigated during the process of defining the M2-F2 configuration.

Aerodynamic Characteristics of the M2-F2 Configuration

Longitudinal aerodynamic characteristics.- The effect on the longitudinal aerodynamic characteristics of varying the Reynolds number from 20×10^6 to 36×10^6 (fig. 4) is seen to be small, particularly for lift coefficients below 0.6. The longitudinal aerodynamic characteristics for various pitch control settings at zero sideslip are presented in figure 5. The trimmed longitudinal aerodynamic characteristics determined from figure 5 are presented in figure 6. It is evident from the results presented in figure 5 that the static stability tends to decrease with increasing lift coefficient (particularly at the higher values of δ_l). The static stability is also decreased slightly

by decreased (more negative) upper flap deflections and decreased lower flap deflections for lift coefficients less than 0.5.

A comparison of figures 5(a) and 5(e) shows that the drag coefficient at zero lift for the minimum flap deflection tested ($\delta_u = 0^\circ$ and $\delta_l = 10^\circ$) was half that for the maximum flap deflection ($\delta_u = -25^\circ$ and $\delta_l = 40^\circ$). This drag increase is indicative of the increase in effective base area as the flaps are deflected away from the body surface. This base area increase results in a maximum untrimmed value of $L/D = 2.1$ when $\delta_u = 25^\circ$ and $\delta_l = 40^\circ$ compared to a value of $L/D = 4.2$ when $\delta_u = 0^\circ$ and $\delta_l = 10^\circ$. A change in maximum L/D of the same magnitude occurs for the trimmed conditions of figure 6 when the cases for $\delta_l = 10^\circ$ and $\delta_l = 40^\circ$ are compared. The maximum trimmed L/D for $\delta_l = 10^\circ$ was 4.0 and the minimum was 2.3 for $\delta_l = 40^\circ$.

Figure 7 indicates that sideslip did not greatly affect the longitudinal characteristics at or below $\beta = 5^\circ$. However, when the angle of sideslip was increased from 5° to 10°, there was a sizable increase in drag and a small reduction in lift curve slope. In addition, at $\beta = 10^\circ$, a definite maximum lift coefficient was reached at $\alpha = 26^\circ$, accompanied by an unstable break in the pitching-moment curve. At $\beta = 0^\circ$ and 5°, a stall break was never reached, and the lift coefficient was a linear function of the angle of attack over the entire range tested ($\alpha = -10^\circ$ to $+28^\circ$).

Lateral-directional aerodynamic characteristics.- These characteristics are presented in figure 8(a) as a function of angle of attack for several sideslip angles and in figure 8(b) as a function of sideslip angle for several angles of attack. These data show that the roll, yaw, and side-force coefficients are nearly linear functions of β. From the yawing-moment results of figure 8(a), there appears to be a transition in the value of the yawing moment due to sideslip (C_{n_β}) from a low value that exists at negative angles of attack to a high value that exists for angles of attack greater than 12°. This could be due to interaction of the vortex flow from the leading edge with the vertical stabilizers. It is also apparent from figure 8(a) that there is sudden change in the yawing and rolling moment at about 26° angle of attack for 10° sideslip. This, together with the previously mentioned unstable break in the pitching-moment curve, suggests that the flow separates on the windward vertical stabilizer and causes a breakdown in the flow over the afterportion of the upper surface and a resulting forward movement of the center of pressure.

The effects of rudder and aileron deflections on the lateral-directional aerodynamic characteristics are presented in figures 9 and 10, respectively, for an upper flap setting of -10° and a lower flap setting of 20°. The variations in rudder and aileron control effectiveness due to longitudinal control settings were negligible; hence, results for only one setting are presented. The lateral-directional aerodynamic characteristics are presented both as functions of angle of attack for different control settings and as functions of control setting for different angles of attack. The effects of the lateral and directional controls are seen to be essentially linear functions of the respective control deflections with only small variations due to angle of attack. The large adverse yawing moment due to roll control ($C_{n_{\delta_a}}/C_{l_{\delta_a}} \approx -1$)

evident in figure 10(b) should be noted. According to the flight test results reported in reference 10, for the M2-F1 vehicle, a $C_{n_{\delta_a}}/C_{l_{\delta_a}}$ value of about -0.2 was obtained during flight tests. This value was considered acceptable for the limited lifting body mission even though the resulting roll response was sluggish and marginal when compared with fighter-type aircraft requirements. Unpublished results of simulator studies of the M2-F2 flight characteristics indicate that its level of adverse yaw could be unacceptable. A center dorsal fin, which reduces the adverse yawing moment due to roll control, is discussed at the end of the following section.

Aerodynamic Characteristics of Various Devices Investigated

Boattail fairing.- The boattail fairing was incorporated into the M2-F2 configuration. The dimensions of the fairing and the model configuration (as it was when the fairing effects were investigated) are shown in figure 3(b). The model was never tested with the aft flaps off when the boattail was off. Because of this, the comparison of the results with and without the boattail fairing includes the effect of moving the aft flap 26 inches farther back from the moment reference. However, this effect is probably a small percentage of the effect of adding the boattail fairing. The basic longitudinal aerodynamic characteristics are shown in figure 11. The results are shown for the elevon on and off and for the aft flaps at -10° incidence. An examination of this figure indicates that the boattail fairing reduced the drag and increased the lift-curve slope, and hence increased the untrimmed maximum L/D by over 0.5. It is also evident from the pitching-moment results of this figure that the longitudinal stability of the M2-F2 was improved by the addition of the boattail fairing. The presence of the elevon affected the contribution of the boattail fairing, especially at low angles of attack.

Elevons.- The elevons were used on the original M2 configuration (designated M2-F1) but not on the M2-F2 configuration. The elevon dimensions and the model configuration (as it was when the elevon effects were investigated) are shown in figure 3(b). (It should be noted that the elevon position tested was different from that of the M2-F1.) The longitudinal aerodynamic characteristics for symmetrical deflections are shown in figure 12(a) and the lateral-directional effects for differential deflections are shown in figure 12(b). These data indicate that the longitudinal aerodynamic characteristics were generally improved by the presence of the elevons. The data shown in figure 12(a) indicate that a 10° change in angle of attack had a greater effect than an equal deflection of the elevon. This suggests that the body-induced upwash, which increases with angle of attack, interacts with the elevons.

The lateral-directional results shown in figure 12(b) indicate that very little yawing moment is produced when the elevons are differentially deflected for roll control, that is, $C_{n_{\delta_a}}/C_{l_{\delta_a}} \approx 0$. Hence, one method of eliminating the large adverse yaw of the M2-F2 configuration previously discussed is to incorporate outboard mounted elevons.

Aft flaps.- The dimensions and arrangement of these flaps are shown in figure 3(b). The control effectiveness of these flaps is compared to that of

the M2-F2 upper flaps in figure 13. It is evident from this figure that changes in lift, drag, and pitching moment are less per degree of flap deflection than are realized with the upper flaps of the M2-F2 configuration even though the tail volumes (tail length times surface area) are almost identical. This is probably due to a greater influence of the M2-F2 flap on the body flow patterns. However, if trimmed results are obtained from these data, drag for a given lift is slightly higher for the upper flaps. Hence, the trim drag is slightly lower for the aft flaps.

Quasi-wings.- The dimensions of the configuration with the wing root faired are given in figure 3(c); the photograph shows the arrangement with the root unfaired and unsealed. The shape of these wings was intended to simulate landing gear doors that could also serve as simple lifting surfaces. The longitudinal aerodynamic characteristics with and without the wings are presented in figure 14.[1] Results are shown for two incidences and with and without the wing root faired and sealed. It is apparent that the quasi-wings improved the performance, especially with the root sealed and faired. The maximum L/D was increased by about 1. These lifting surfaces would not only improve the performance but would also reduce the landing attitude substantially. For a 5.2° wing incidence at $C_L = 0.5$, the wings would reduce α by about 7.5°. The maximum incremental increase in C_L achieved for the range of variables investigated was 0.22 at $\alpha = 9^{\circ}$. This is equivalent to a maximum lift coefficient of 1.1 based on the projected area of the wing and is an unusually high value for this type of lifting surface. These results suggest that this type of lifting device is a promising method of improving the performance of lifting body vehicles.

A simple computation using the results of figure 14 shows that the center of pressure of the resultant force increment moves forward of the wing panels after wing stall occurs. This indicates significant interactions between the flow about the basic body and the quasi-wing panels.

Outboard ventral fins.- The outboard ventral fins are described in figure 3(d). These fins were intended to straighten the outboard flow that occurred on the lower surface of the body. Two configurations were investigated, the thin outboard ventral fins and the thick outboard ventral fins. The thick fins were designed to withstand high-speed aerodynamic heating.

The aerodynamic characteristics are shown in figure 15 for the thin fins and in figure 16 for the thick fins. It is seen that the thin fins increase both the longitudinal and directional stability and slightly decrease the rolling moment due to sideslip. The aerodynamic effects of the thick fins are similar but smaller than those of the thin fins.

Center dorsal fin.- The center dorsal fin described in figure 3(d) was intended as a flow straightening device during aileron control settings. The lateral-directional aerodynamic characteristics are shown in figure 17 as a function of roll control settings. The basic longitudinal and lateral-directional aerodynamic characteristics are not presented since the effect of

[1]The scatter in the moment coefficient evident in figure 14 and in figures 11 and 12 is a result of the reduced accuracy due to the low test dynamic pressure (17 lb/ft^2).

the dorsal fin on these characteristics was negligible. The results of figure 17 indicate that $C_{n_{\delta_a}}/C_{l_{\delta_a}}$ would be reduced from about -1 to -0.2 if the dorsal fin were used on the M2-F2. The effect on the roll control was very small. Hence, if the large adverse yaw due to roll control present on the M2-F2 configuration is unacceptable, one successful method of markedly decreasing it is by a dorsal fin such as that tested.

CONCLUDING REMARKS

The maximum untrimmed L/D of the M2-F2 configuration was 4.2; the maximum trimmed L/D was 4.0. The model had positive static longitudinal stability over the entire trim range investigated.

The adverse yaw due to roll control was large but can be reduced by the addition of a small dorsal fin between the upper flaps.

Wind-tunnel tests of the M2-F2 lifting body have shown that there are significant interactions between the components and the body. Thus, the aerodynamic characteristics determined from tests of isolated components could not be superimposed to predict the overall aerodynamic characteristics accurately.

Ames Research Center
National Aeronautics and Space Administration
Moffett Field, Calif., Nov. 3, 1966
124-07-02-10-21

REFERENCES

1. Kenyon, George C.; and Edwards, George G.: A Preliminary Investigation of Modified Blunt 13° Half-Cone Re-entry Configurations at Subsonic Speeds. NASA TM X-501, 1961.

2. Rakich, John V.: Supersonic Aerodynamic Performance and Static-Stability Characteristics of Two Blunt-Nosed Modified 13° Half-Cone Configurations. NASA TM X-375, 1960.

3. Dennis, David H.; and Edwards, George G.: The Aerodynamic Characteristics of Some Lifting Bodies. NASA TM X-376, 1960.

4. Kenyon, George C.; and Sutton, Fred B.: The Longitudinal Aerodynamic Characteristics of a Re-entry Configuration Based on a Blunt 13° Half-Cone at Mach Numbers to 0.92. NASA TM X-571, 1961.

5. Rakich, John V.: Aerodynamic Performance and Static-Stability Characteristics of a Blunt-Nosed Boattailed 13° Half-Cone at Mach Numbers From 0.6 to 5.0. NASA TM X-570, 1961.

6. Kenyon, George C.: The Lateral and Directional Aerodynamic Characteristics of a Re-entry Configuration Based on a Blunt 13° Half-Cone at Mach Numbers to 0.90. NASA TM X-583, 1961.

7. Axelson, John A.: Pressure Distributions for the M-2 Lifting Entry Vehicle at Mach Numbers of 0.23, 5.2, 7.4, and 10.4. NASA TM X-997, 1964.

8. Horton, Victor W.; Eldredge, Richard C.; and Klein, Richard E.: Flight-Determined Low-Speed Lift and Drag Characteristics of the Lightweight M2-F1 Lifting Body. NASA TN D-3021, 1965.

9. Mort, Kenneth W.; and Gamse, Berl: Full-Scale Wind-Tunnel Investigation of the Longitudinal Aerodynamic Characteristics of the M2-F1 Lifting Body Flight Vehicle. NASA TN D-3330, 1966.

10. Smith, Harriet J.: Evaluation of the Lateral-Directional Stability and Control Characteristics of the Lightweight M2-F1 Lifting Body at Low Speeds. NASA TN D-3022, 1965.

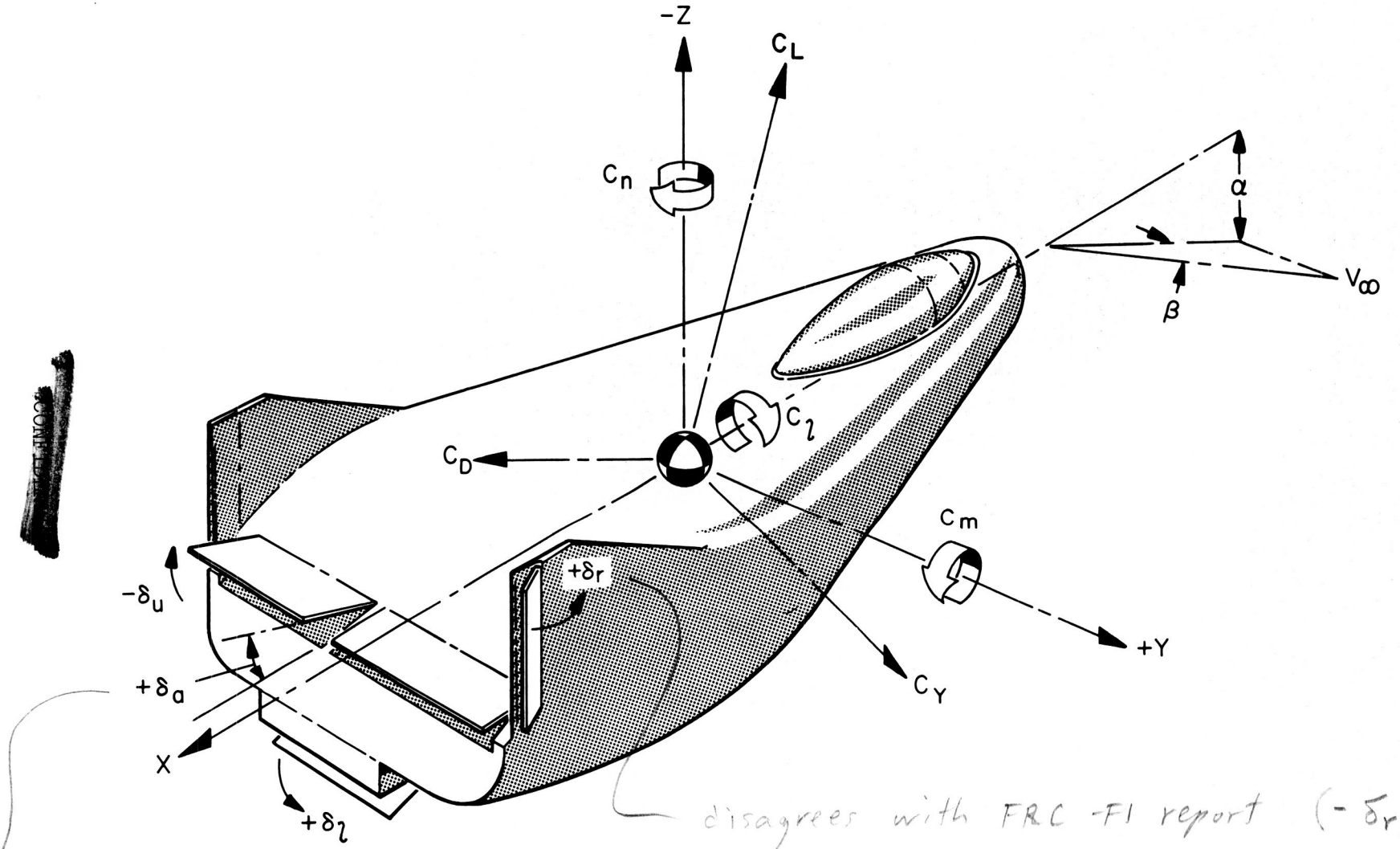

Figure 1.- Sign conventions.

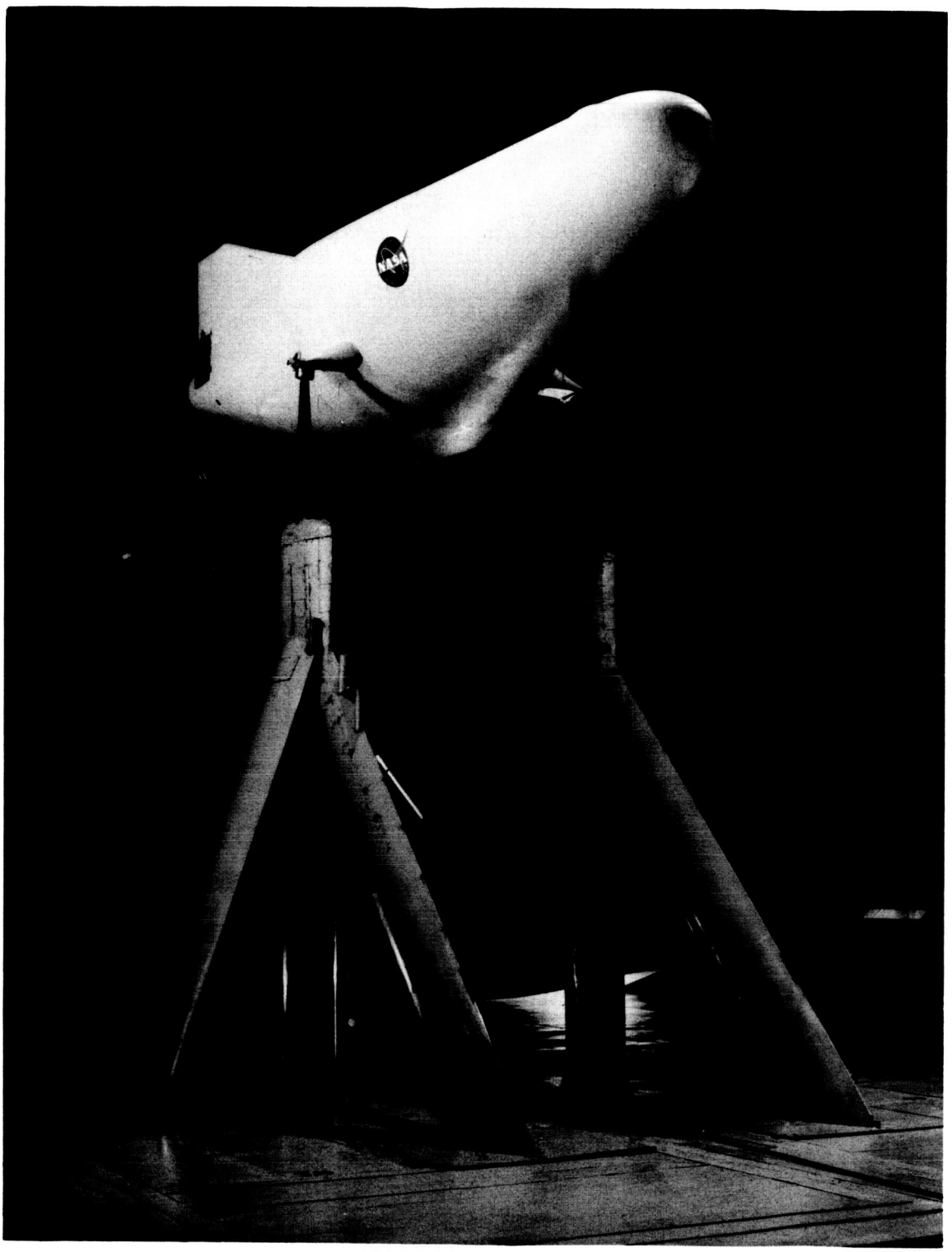

(a) Three-quarter front view. A-32524

Figure 2.- The model mounted in the 40- by 80-foot wind tunnel.

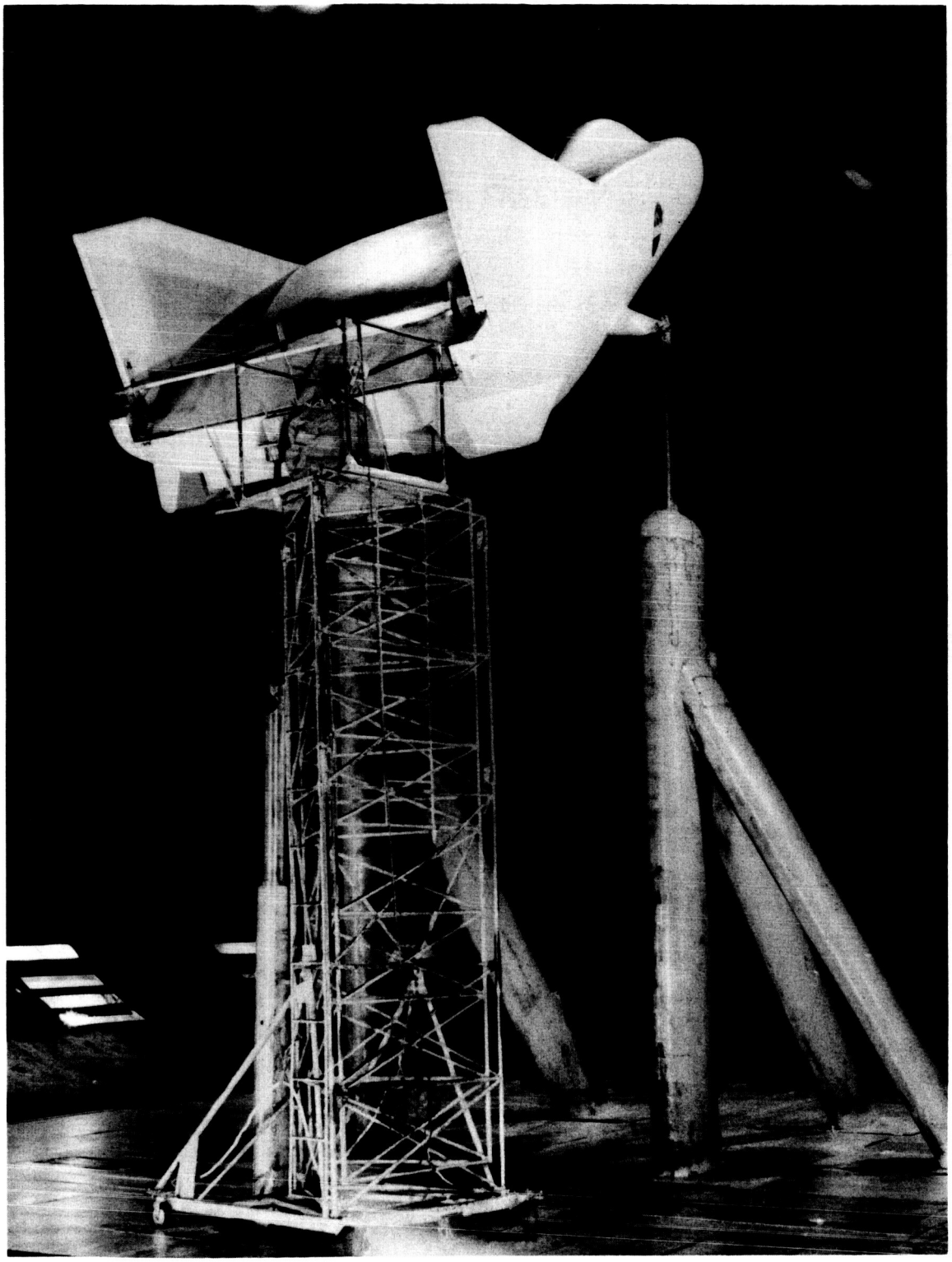

A-33440

(b) Three-quarter rear view.

Figure 2.- Concluded.

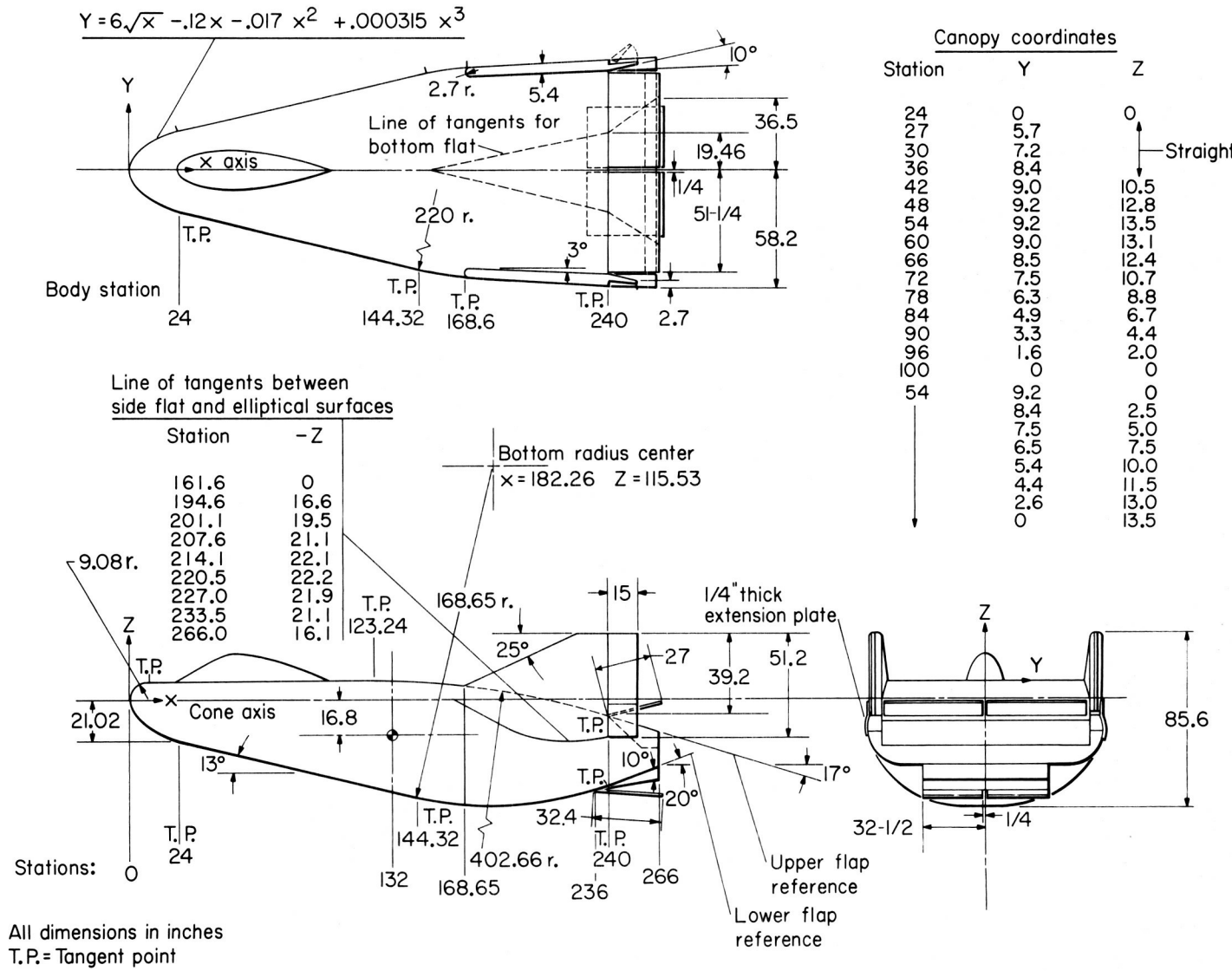

(a) Basic M2-F2 configuration.

Figure 3.- Model dimensions.

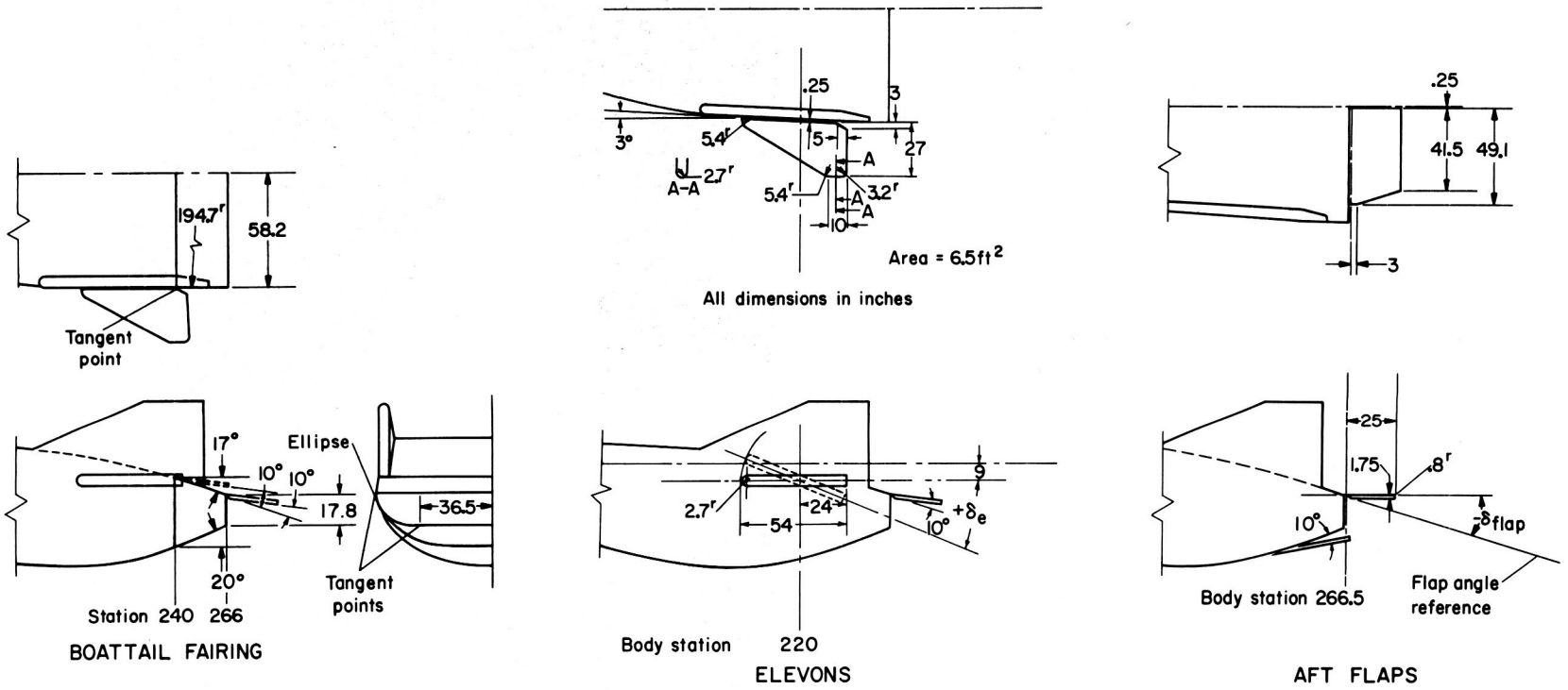

(b) Details of boattail fairing, elevons, and aft flaps.

Figure 3.- Continued.

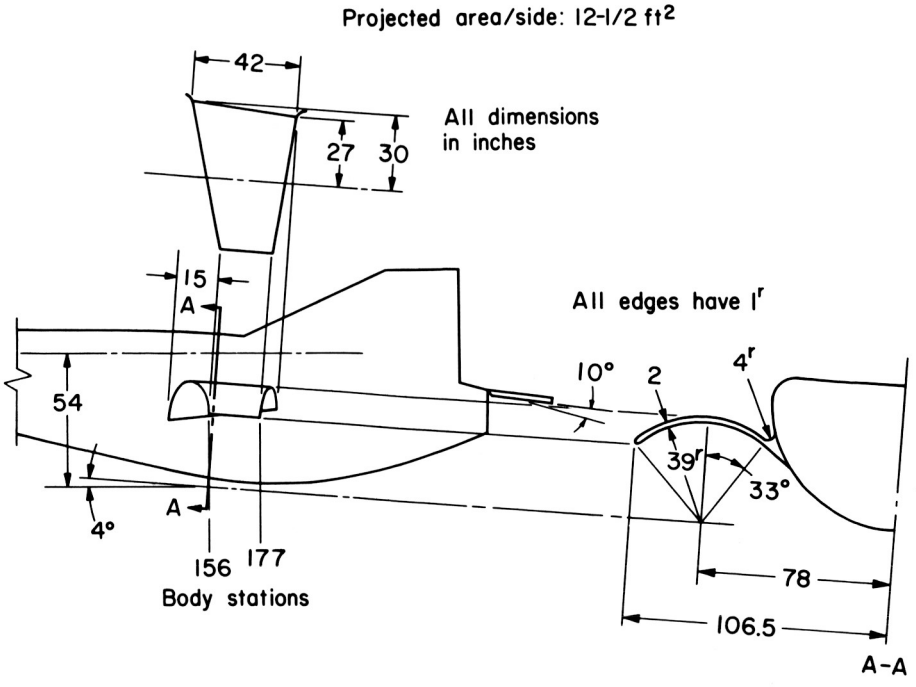

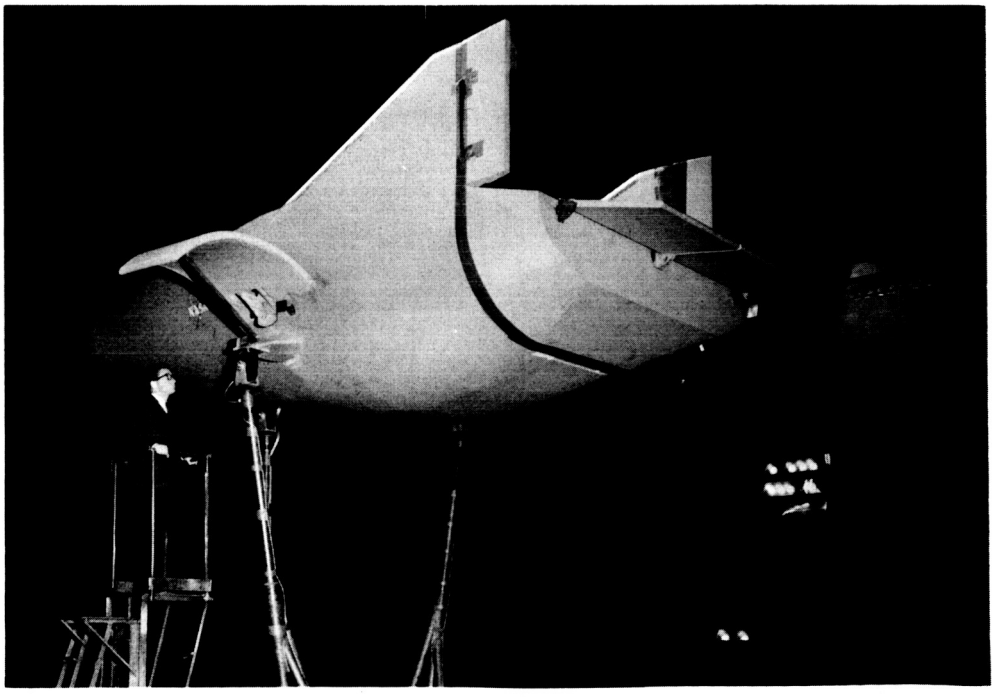

A-31466

(c) Details of quasi-wings.

Figure 3.- Continued.

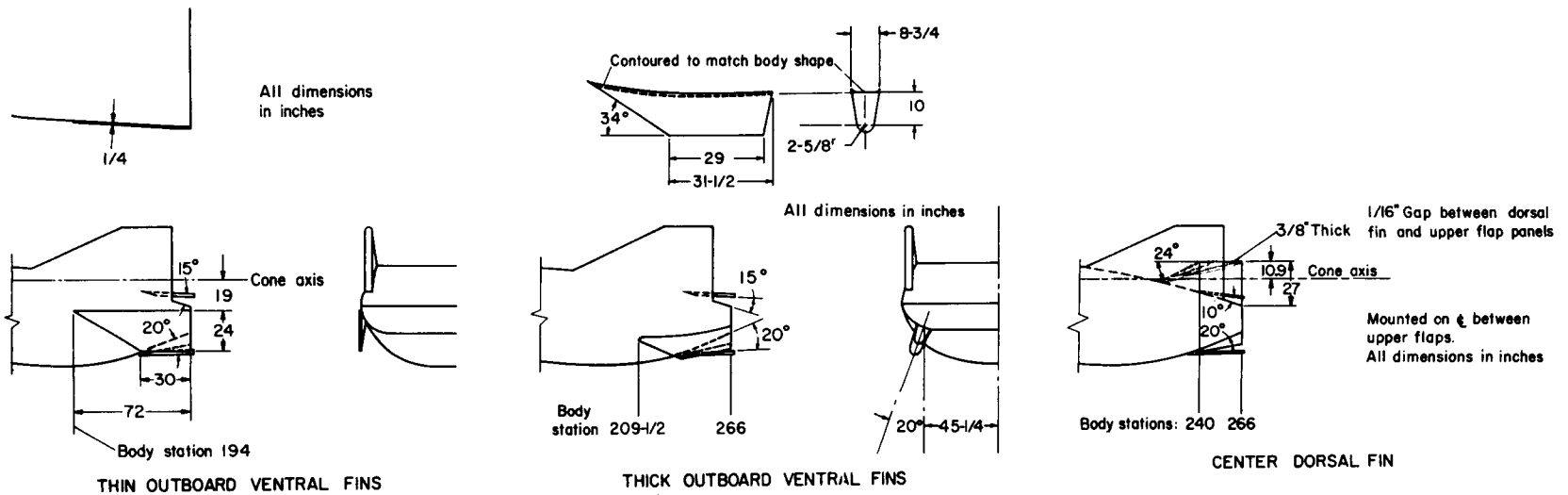

(d) Details of outboard ventral fins and center dorsal fin.

Figure 3.- Concluded.

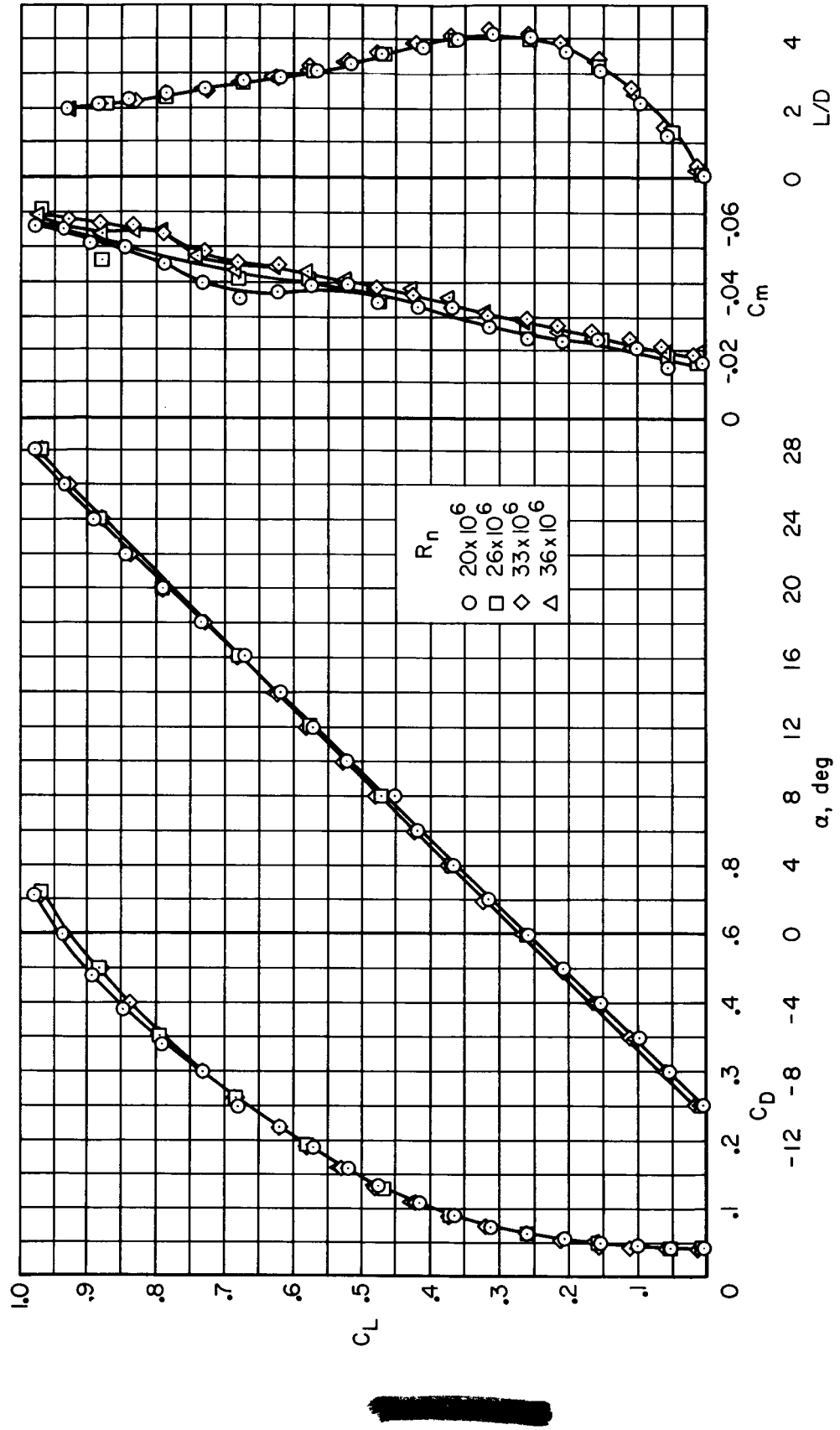

Figure 4.- The effect of Reynolds number on the longitudinal aerodynamic characteristics of the basic M2-F2 configuration; $\delta_u = 0^o$, $\delta_l = 20^o$.

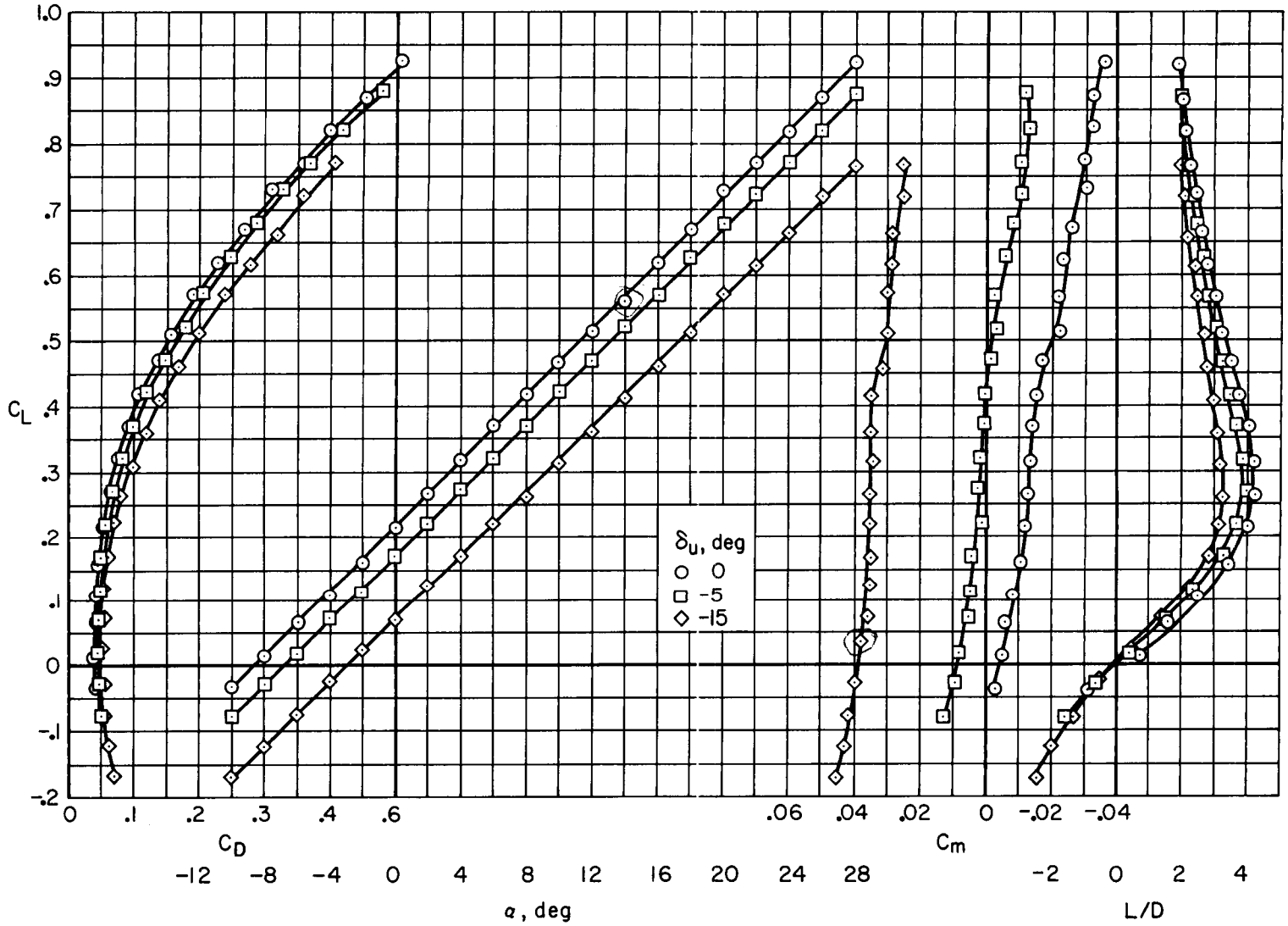

(a) $\delta_l = 15^o$.

Figure 5.- The longitudinal aerodynamic characteristics of the basic M2-F2 configuration at $\beta = 0^o$.

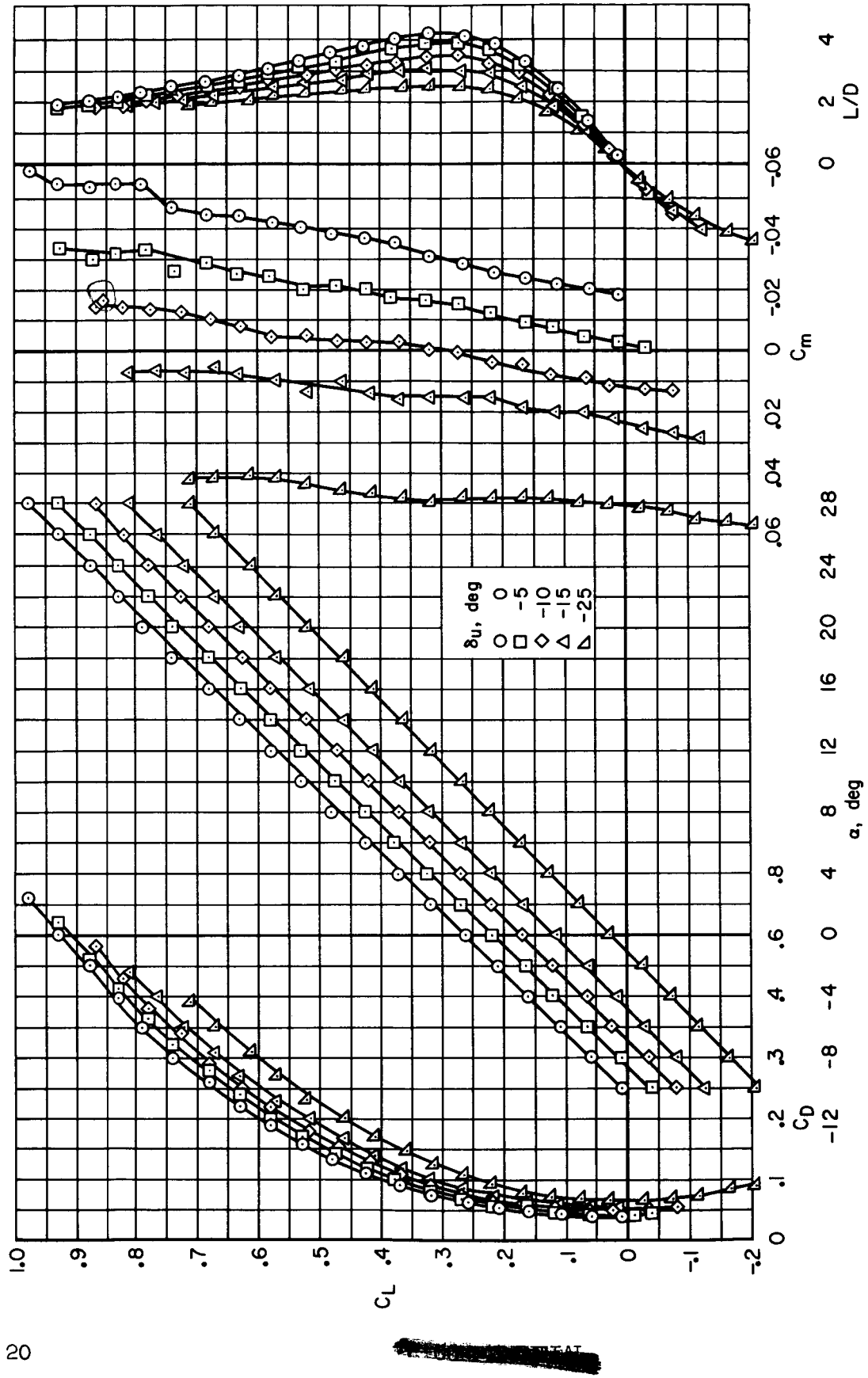

(b) $\delta_l = 15^\circ$.

Figure 5.- Continued.

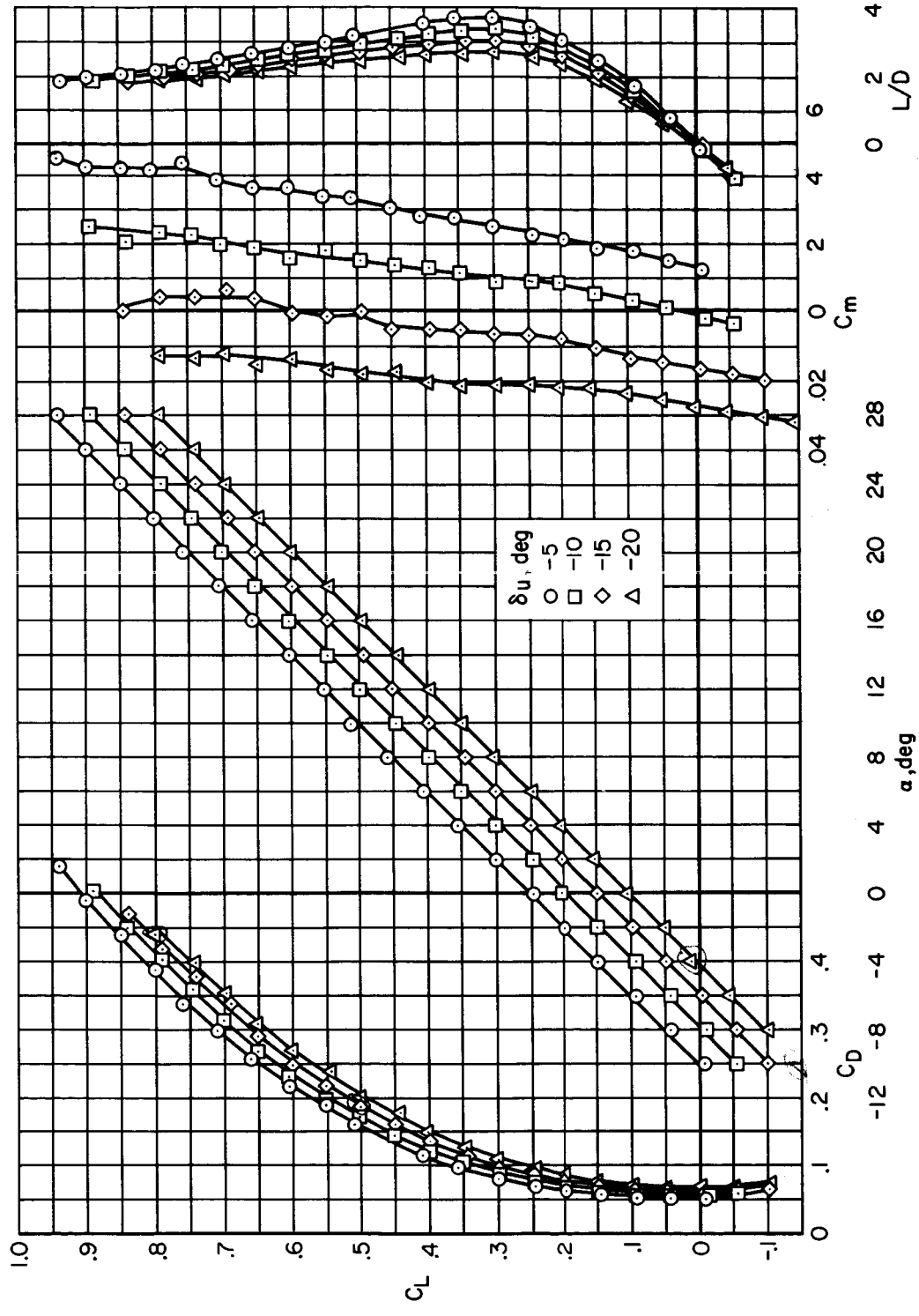

(c) $\delta_l = 25^\circ$.

Figure 5.- Continued.

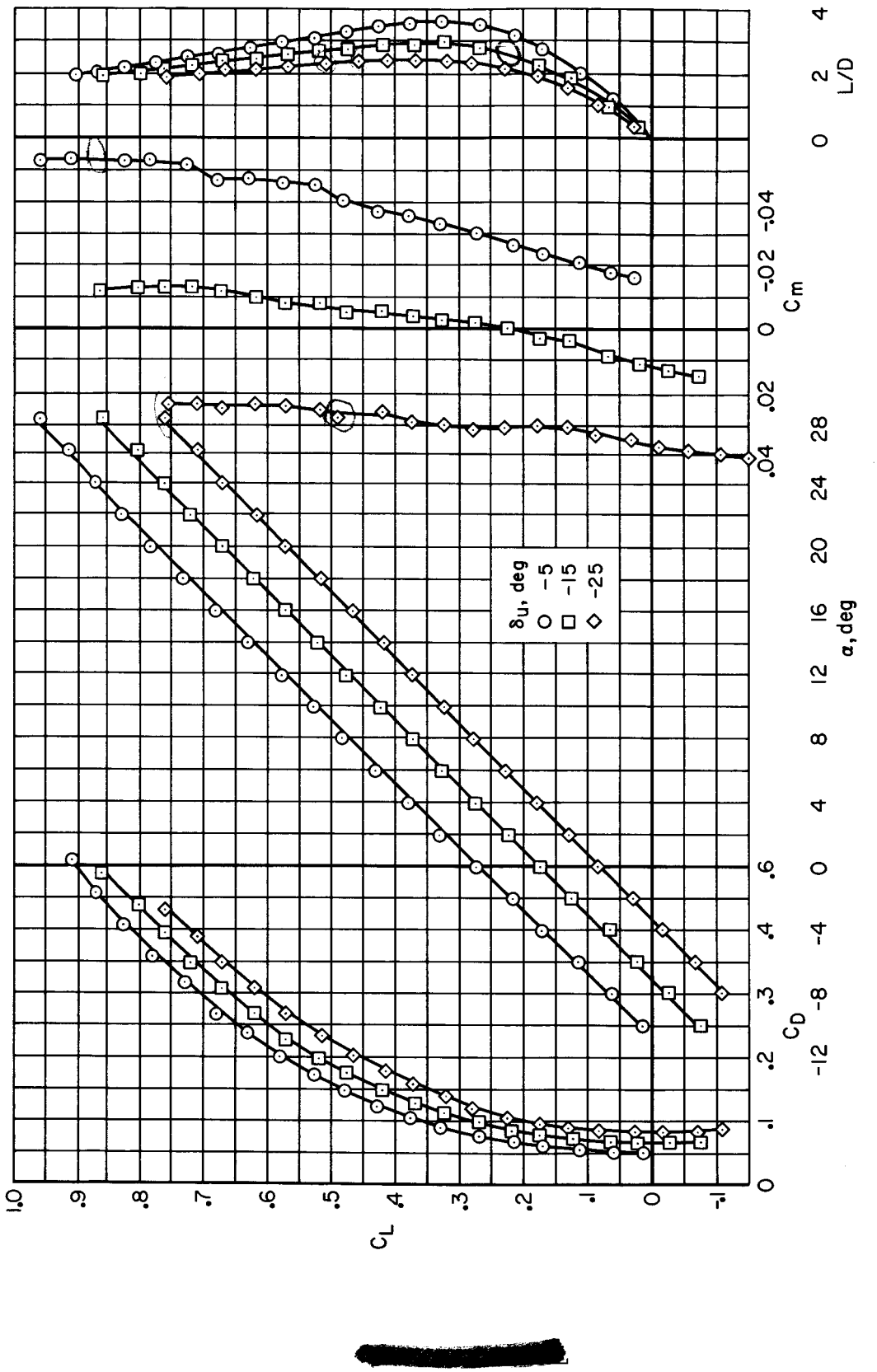

(d) $\delta_l = 30^\circ$.

Figure 5.- Continued.

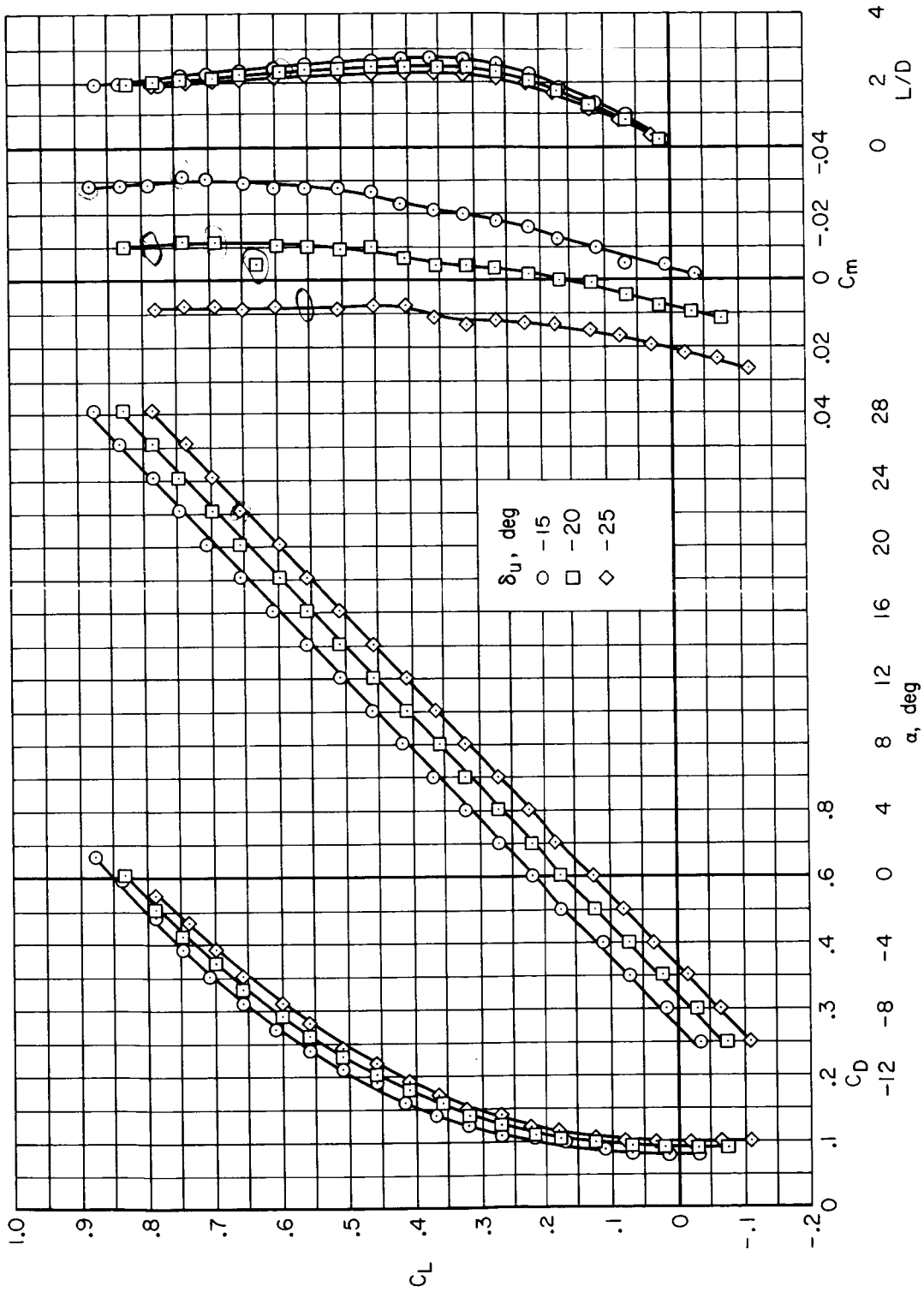

(e) $\delta_\ell = 40°$.

Figure 5.- Concluded.

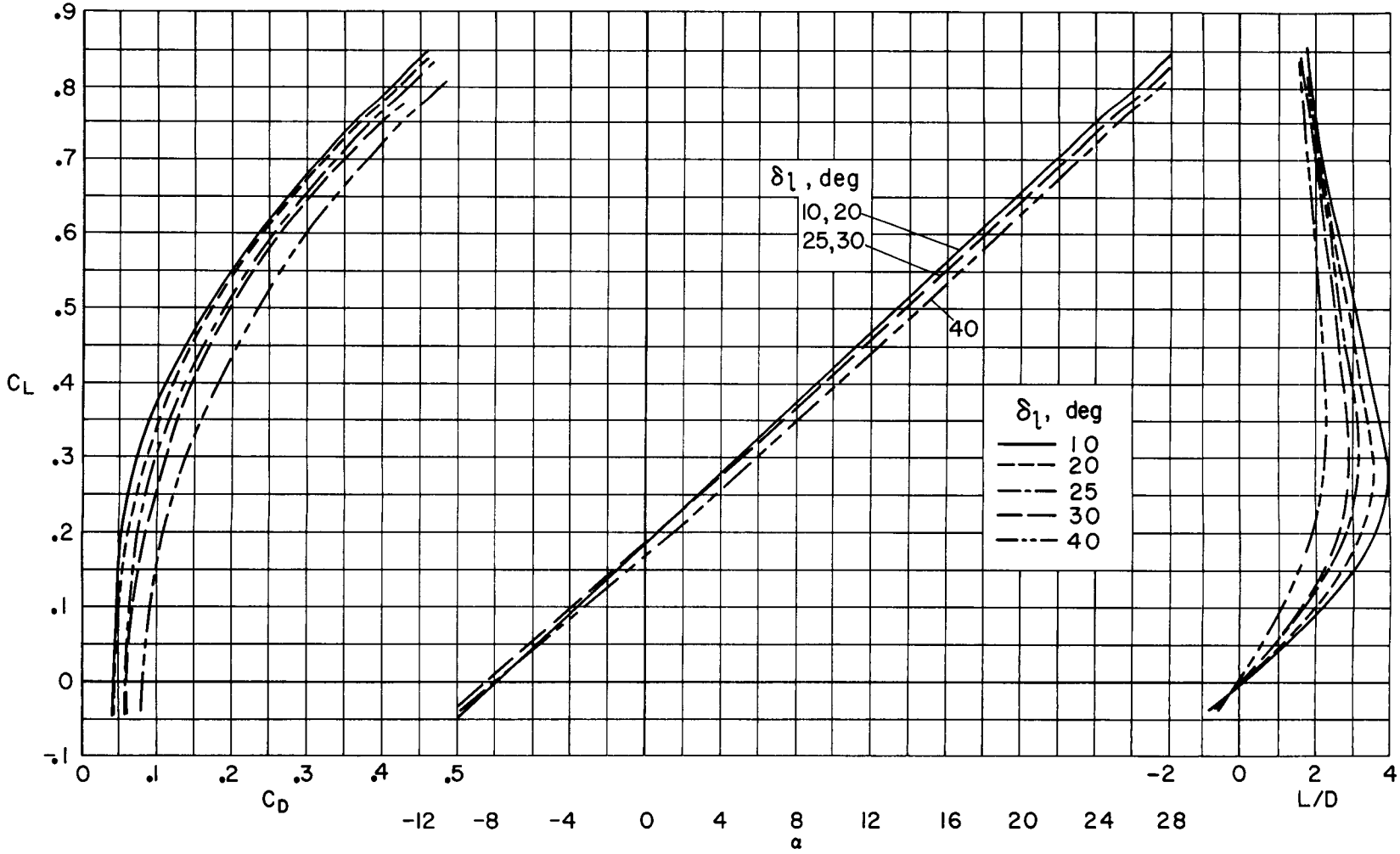

(a) Basic longitudinal aerodynamic characteristics.

Figure 6.- Results at longitudinally trimmed conditions for the basic M2-F2 configuration.

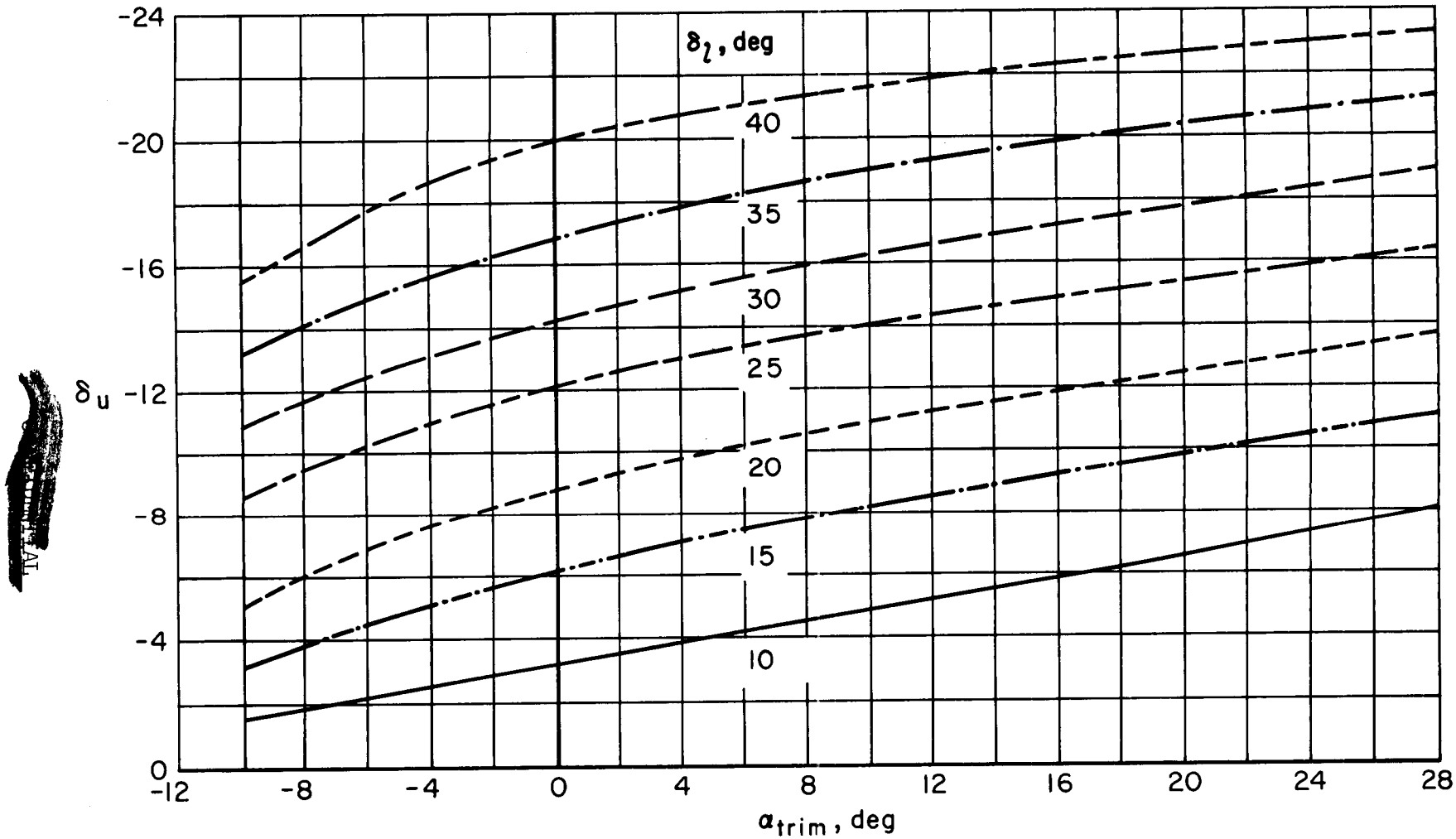

(b) Flap deflection combinations required.

Figure 6.- Concluded.

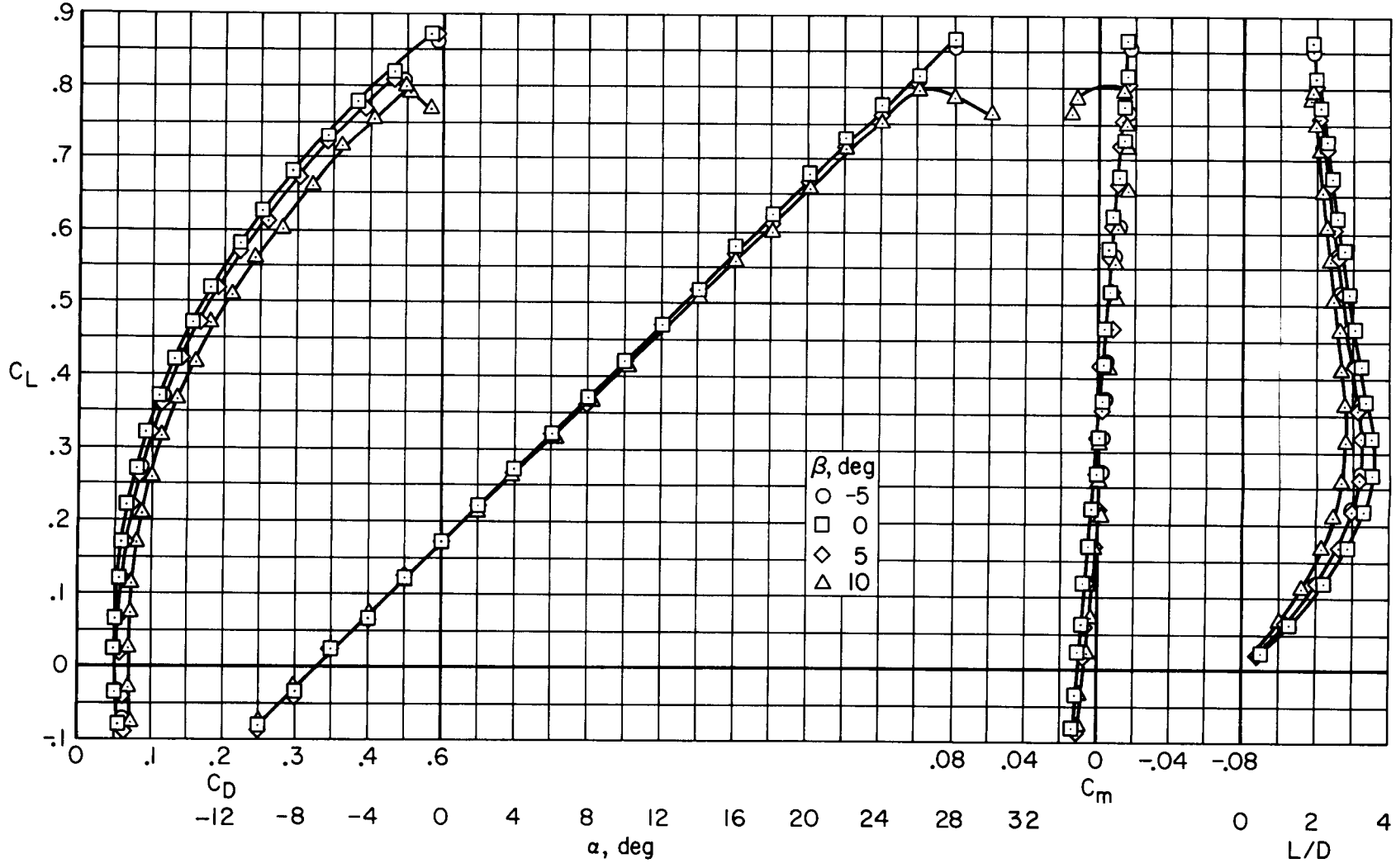

Figure 7.- Effects of sideslip on the longitudinal aerodynamic characteristics of the basic M2-F2 configuration; $\delta_u = -10^\circ$, $\delta_l = 20^\circ$.

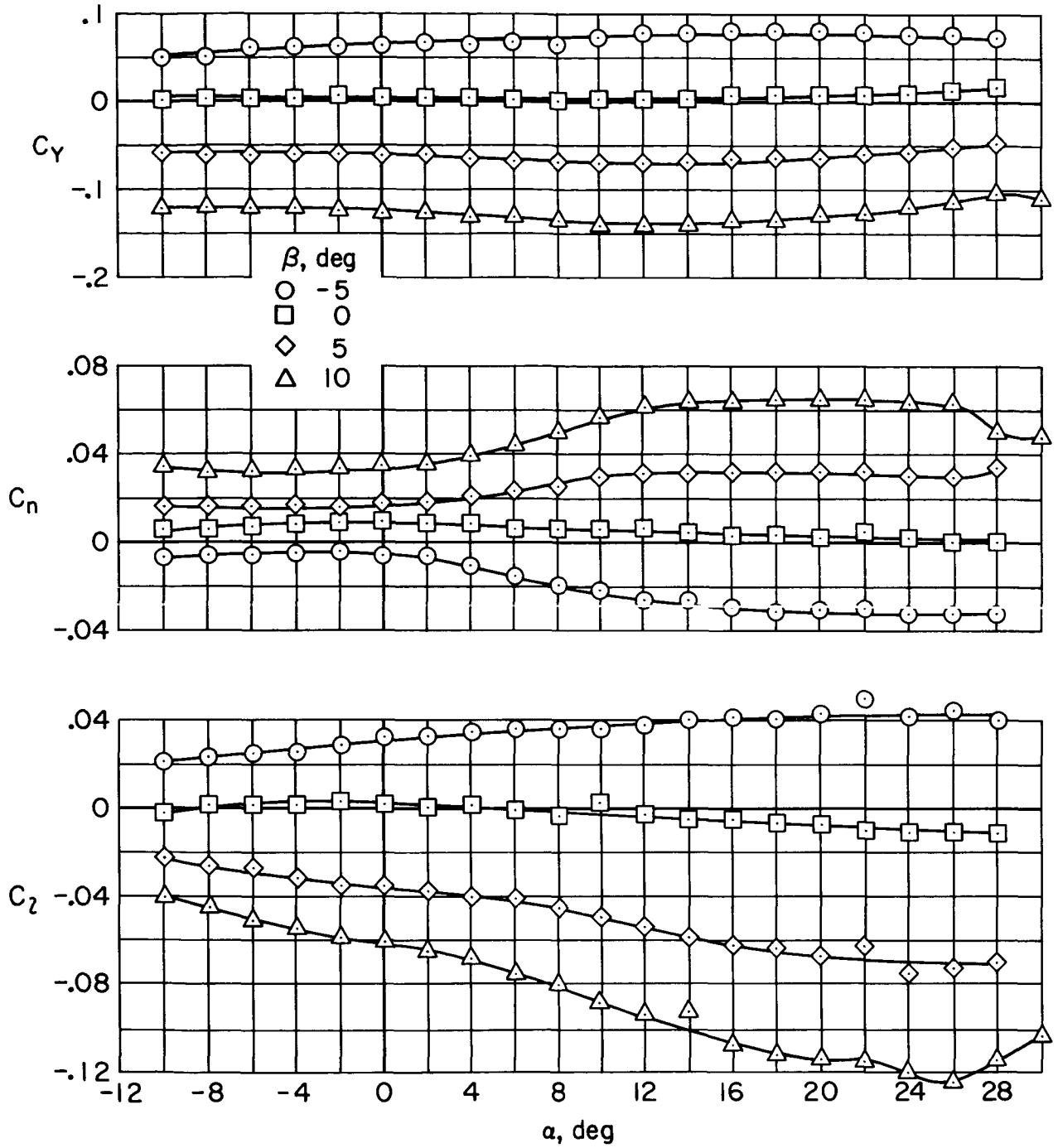

(a) Results presented as a function of α.

Figure 8.- Effects of sideslip on the lateral-directional aerodynamic characteristics of the basic M2-F2 configuration; $\delta_u = -10^\circ$, $\delta_l = 20^\circ$.

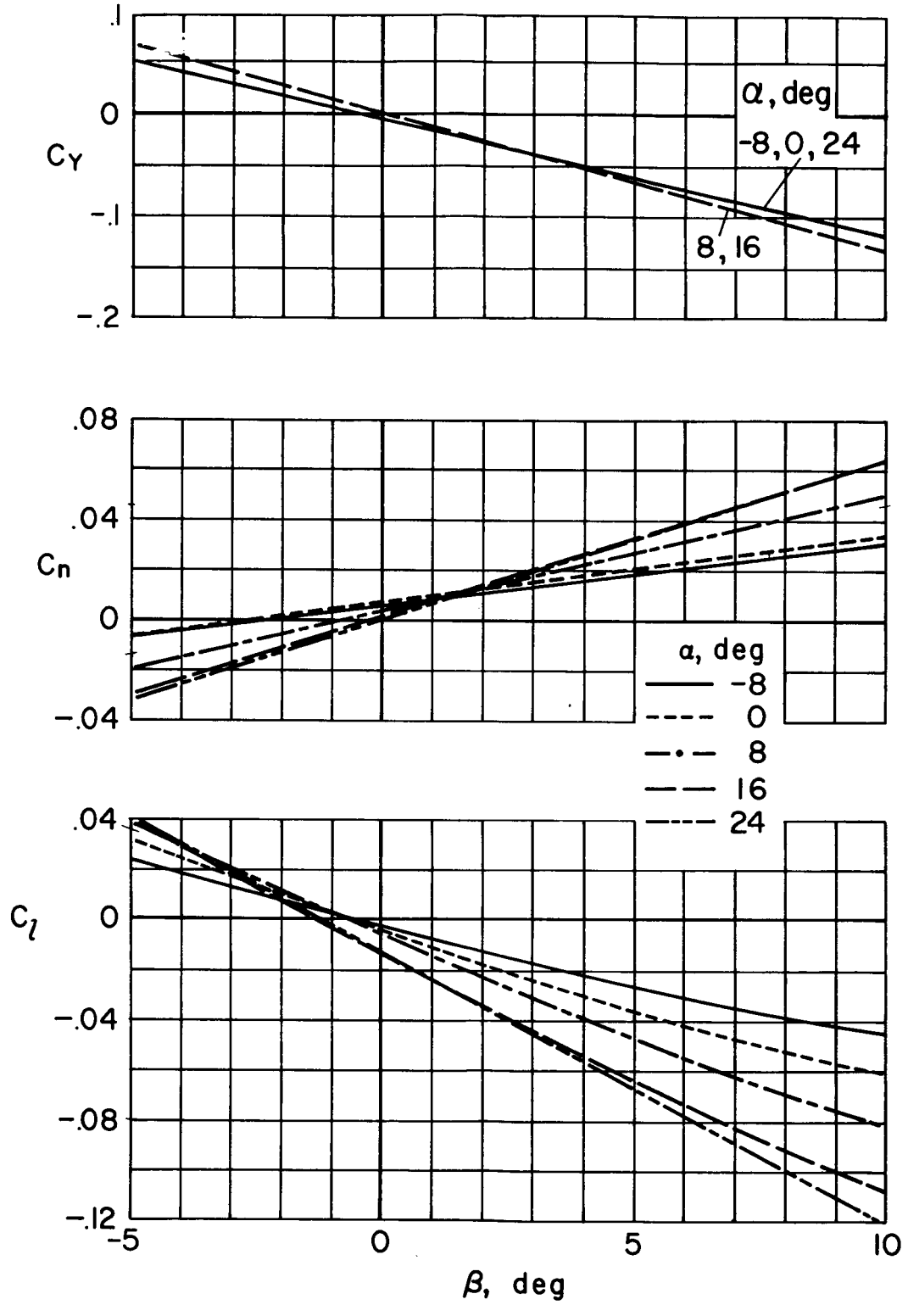

(b) Results presented as a function of β.

Figure 8.- Concluded.

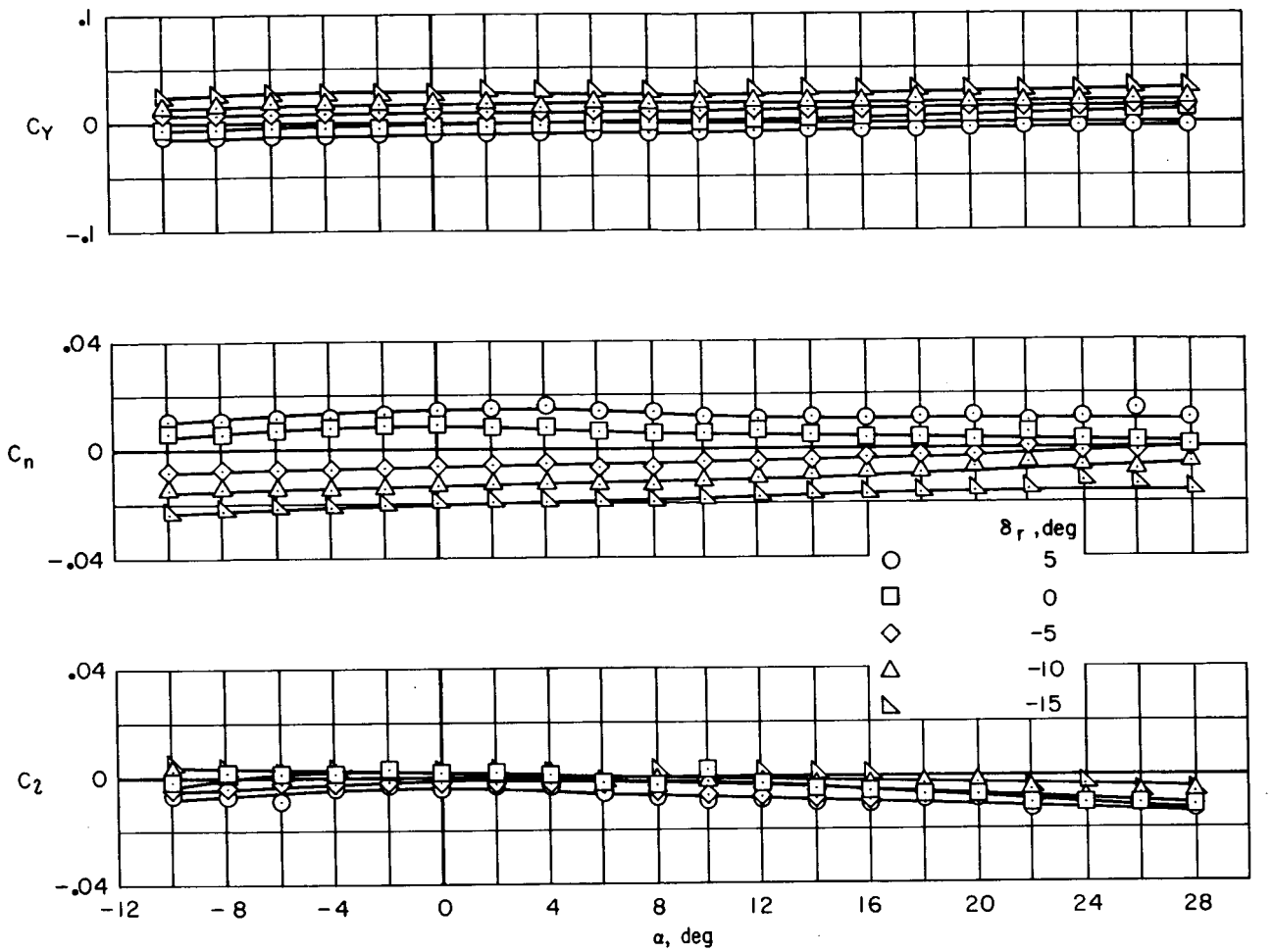

(a) Results presented as a function of α.

Figure 9.- Effects of rudder deflection on the lateral-directional aerodynamic characteristics of the basic M2-F2 configuration; $\delta_u = -10^\circ$, $\delta_l = 20^\circ$.

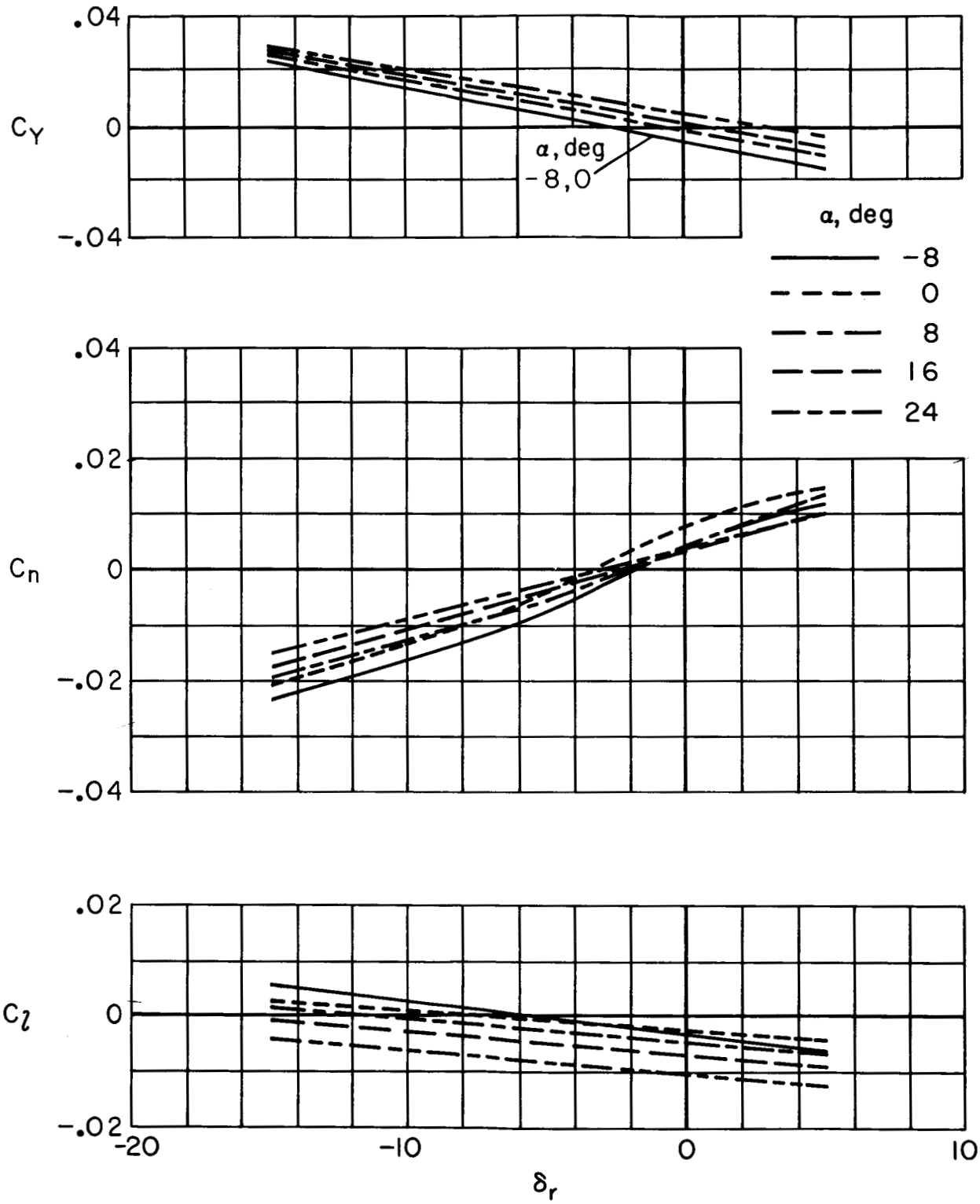

(b) Results presented as a function of δ_r.

Figure 9.- Concluded.

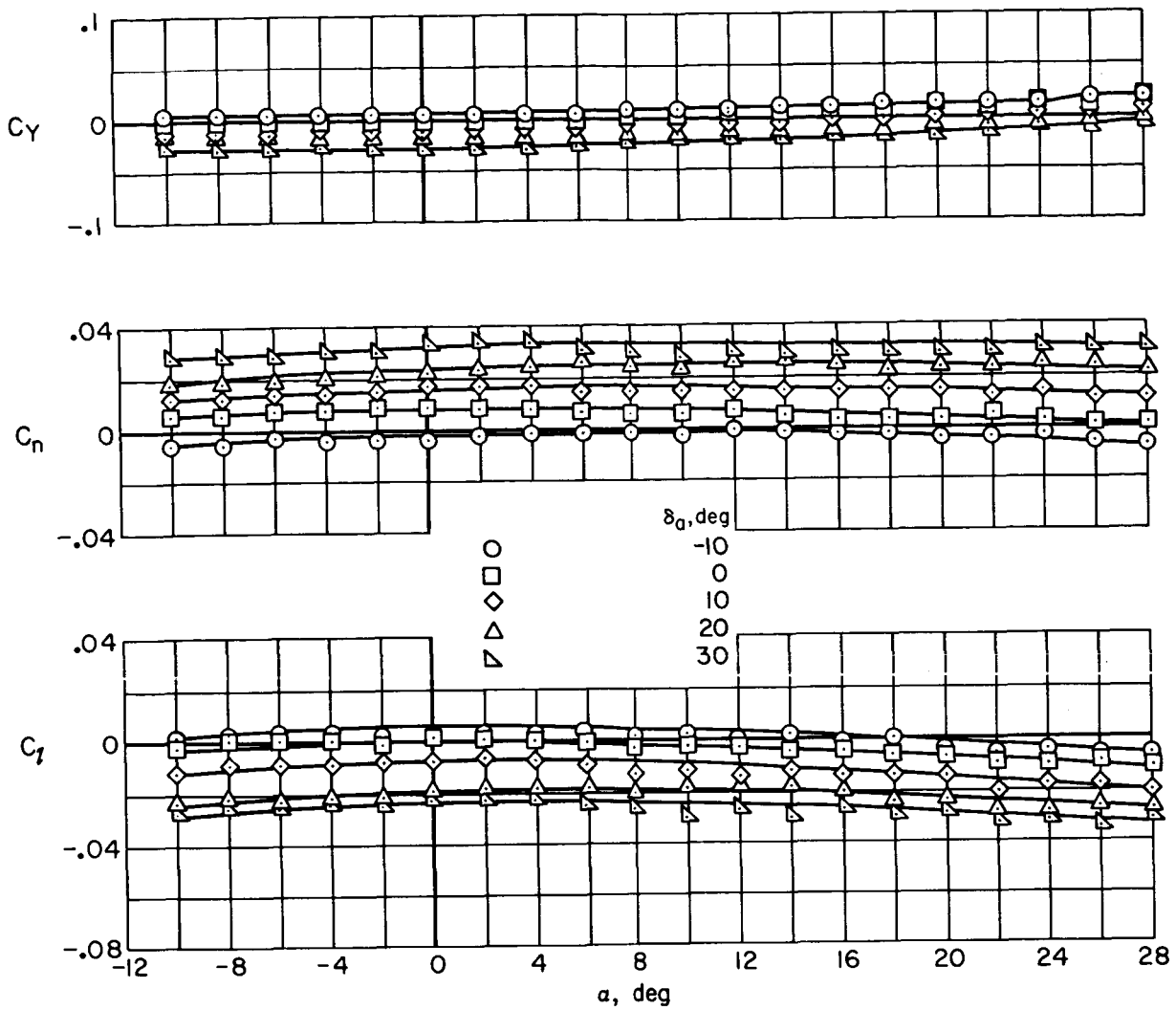

(a) Results presented as a function of α.

Figure 10.- Effects of aileron deflection on the lateral-directional aerodynamic characteristics of the basic M2-F2 configuration; $\delta_u = -10^\circ$, $\delta_l = 20^\circ$.

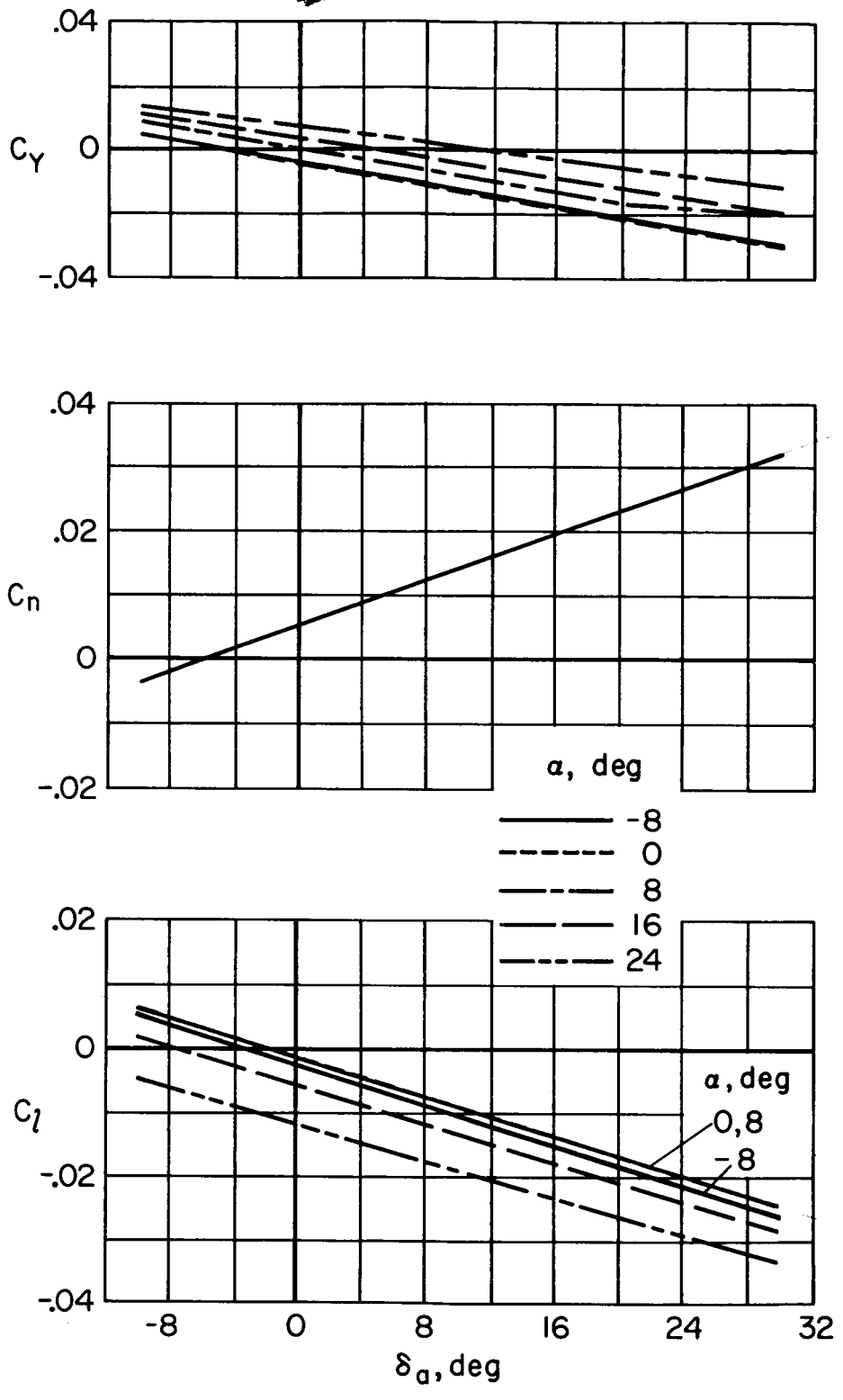

(b) Results presented as a function of δ_a.

Figure 10.- Concluded.

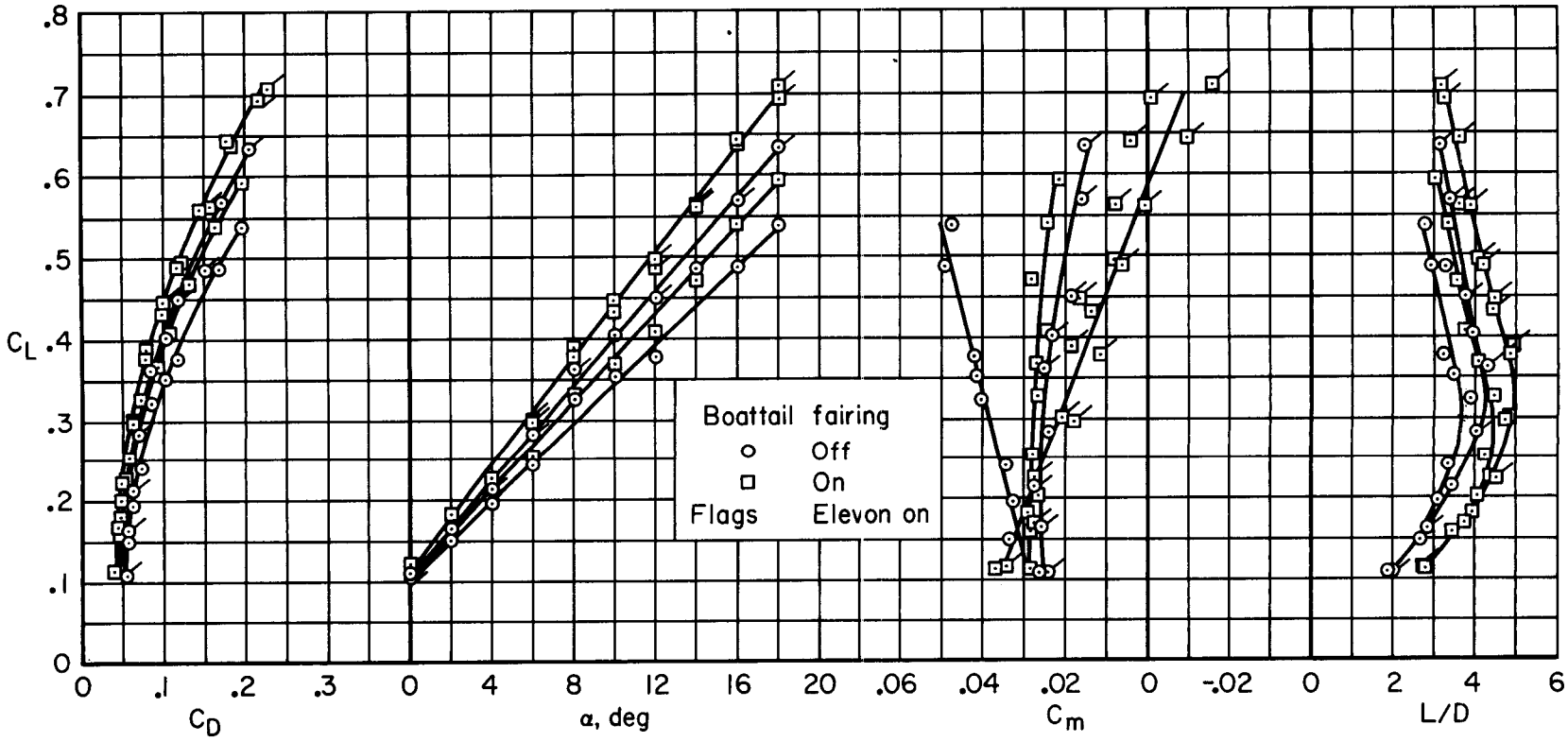

Figure 11.- The effect of the boattail fairing on the longitudinal aerodynamic characteristics at $q = 17$ lb/ft^2; aft flaps on at -10° incidence, upper and lower flaps off.

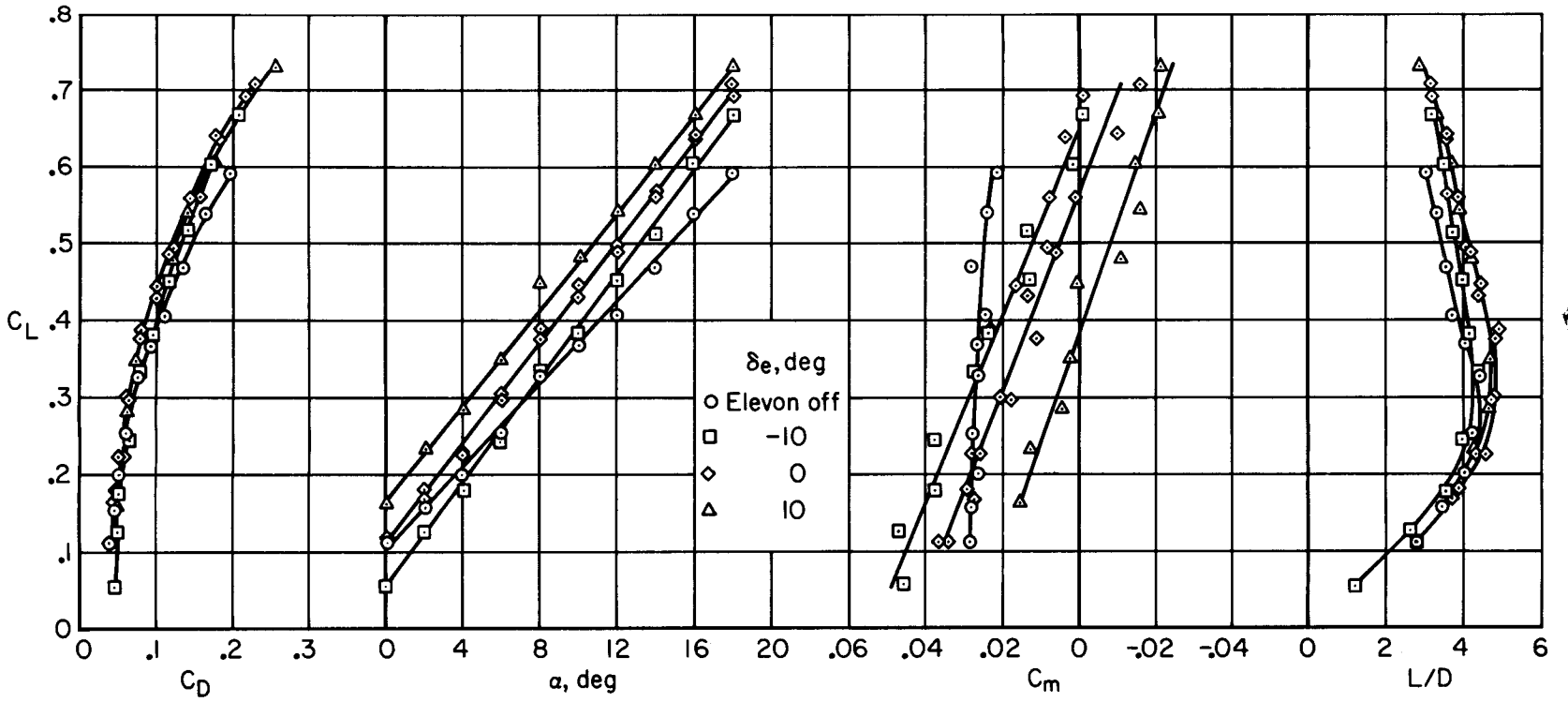

(a) Longitudinal aerodynamic characteristics.

Figure 12.- The effect of the elevons with the boattail on, aft flaps at -10° incidence, and $q = 17$ lb/ft^2; upper and lower flaps off.

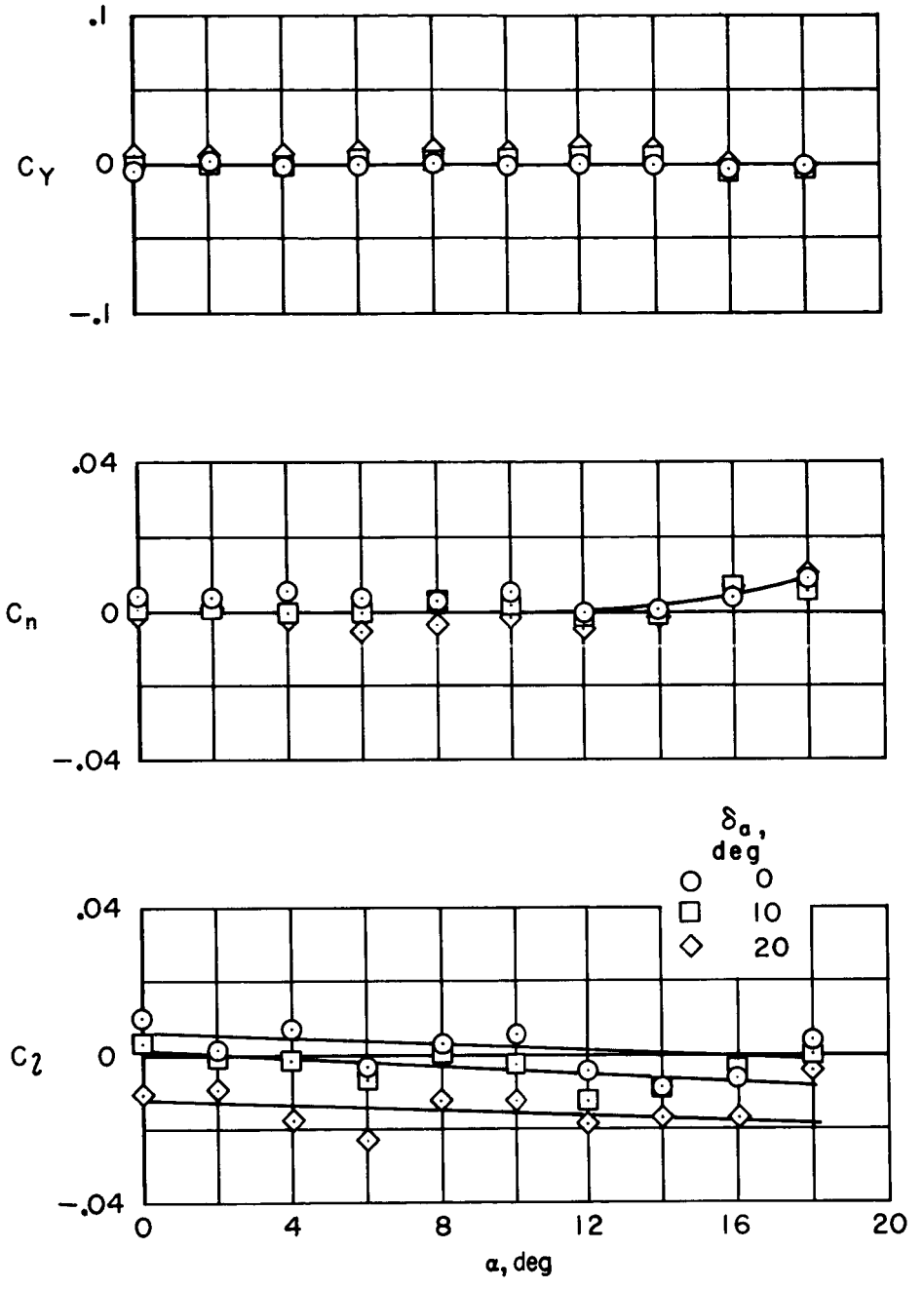

(b) Lateral-directional aerodynamic characteristics for three lateral control settings of elevons.

Figure 12.- Concluded.

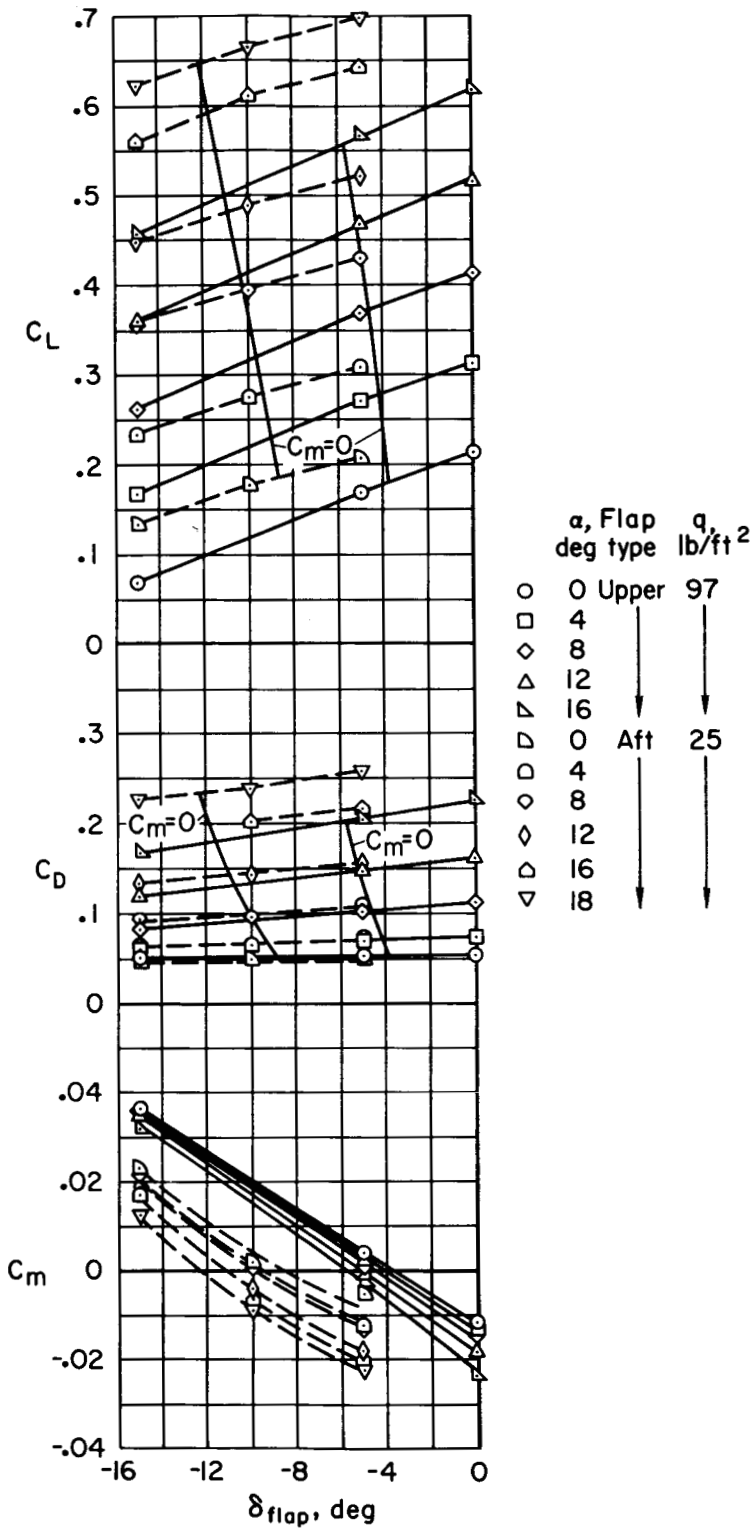

Figure 13.- Comparison of aft flap control effectiveness with upper flap control effectiveness; $\delta_l = 10^\circ$.

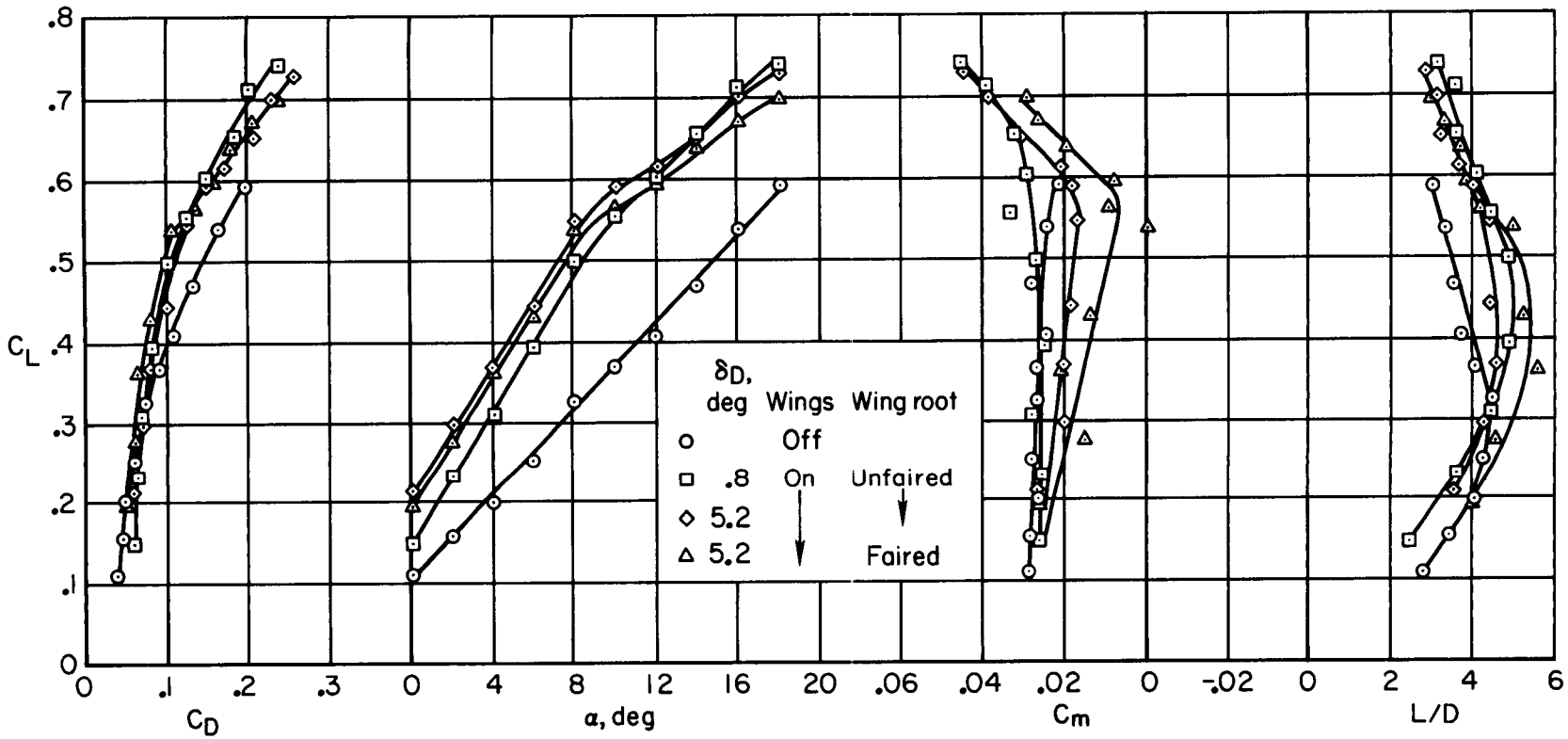

Figure 14.- The effects of the small wings resembling landing gear doors on the longitudinal aerodynamic characteristics; aft flaps at -10° incidence, δ_l = 10°, and q = 17 lb/ft^2.

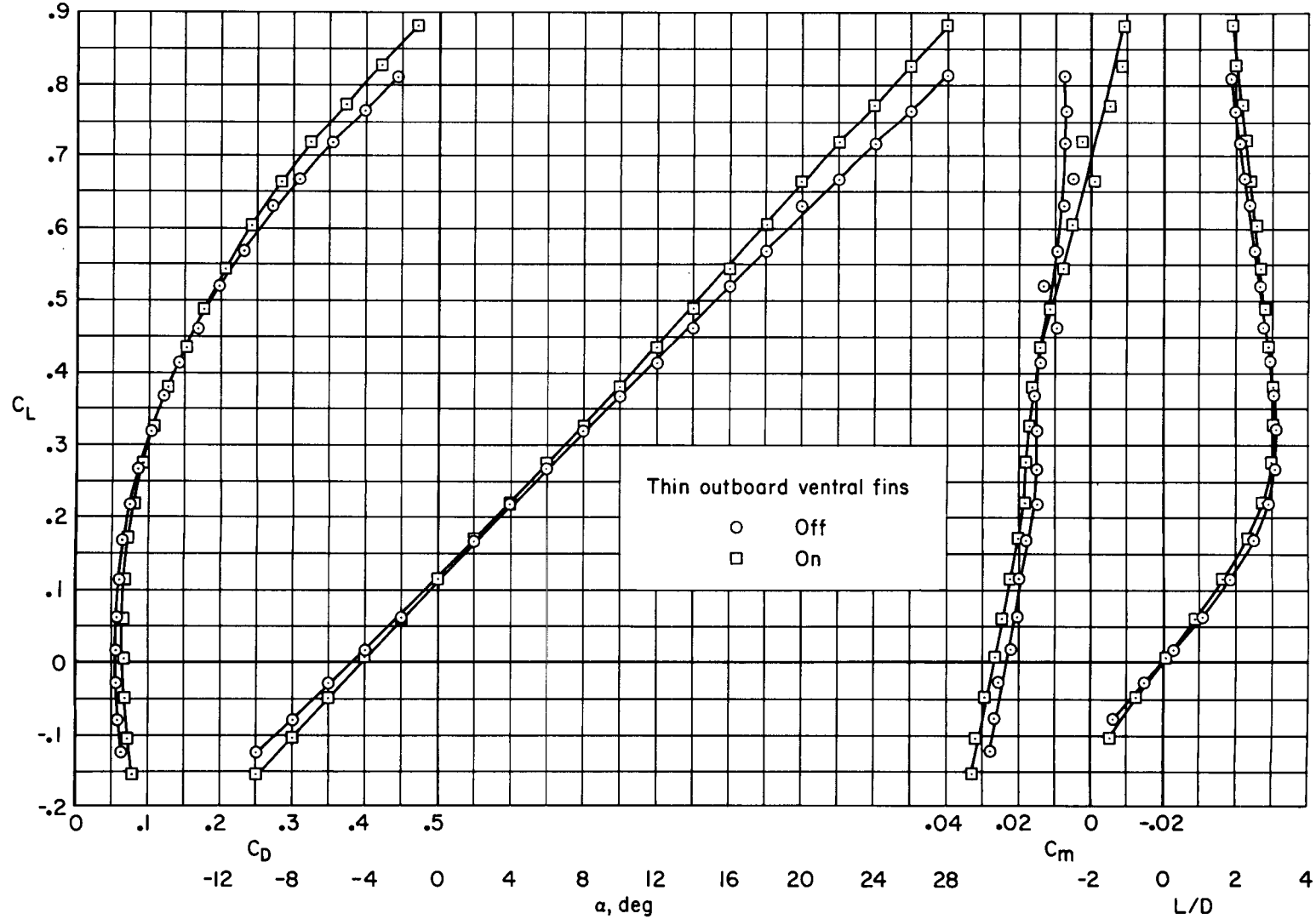

(a) Longitudinal aerodynamic characteristics.

Figure 15.- The effects of the thin outboard fins on the aerodynamic characteristics of the basic M2-F2 configuration; $\delta_u = -15^\circ$, $\delta_l = 20^\circ$.

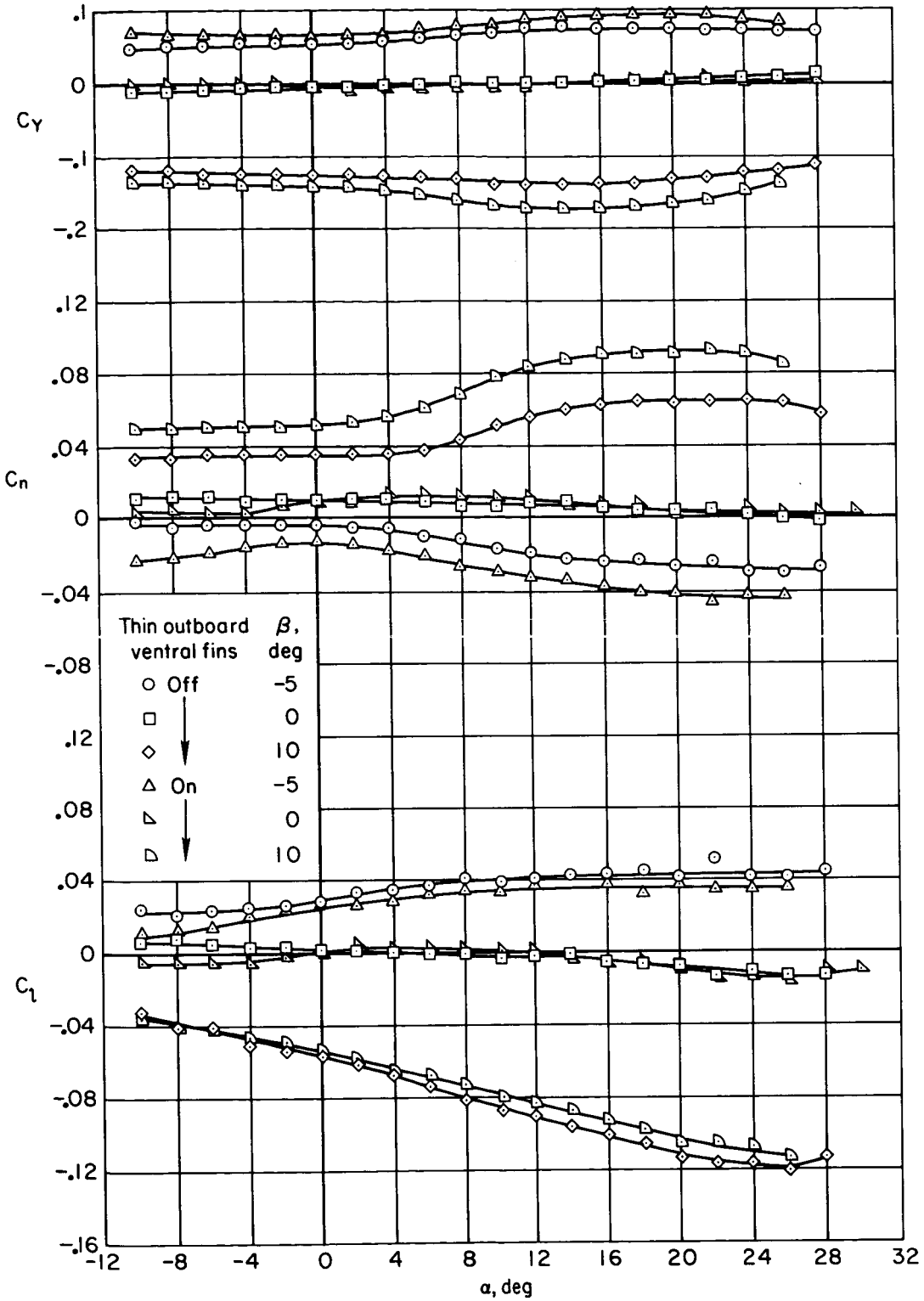

(b) Lateral-directional aerodynamic characteristics.

Figure 15.- Concluded.

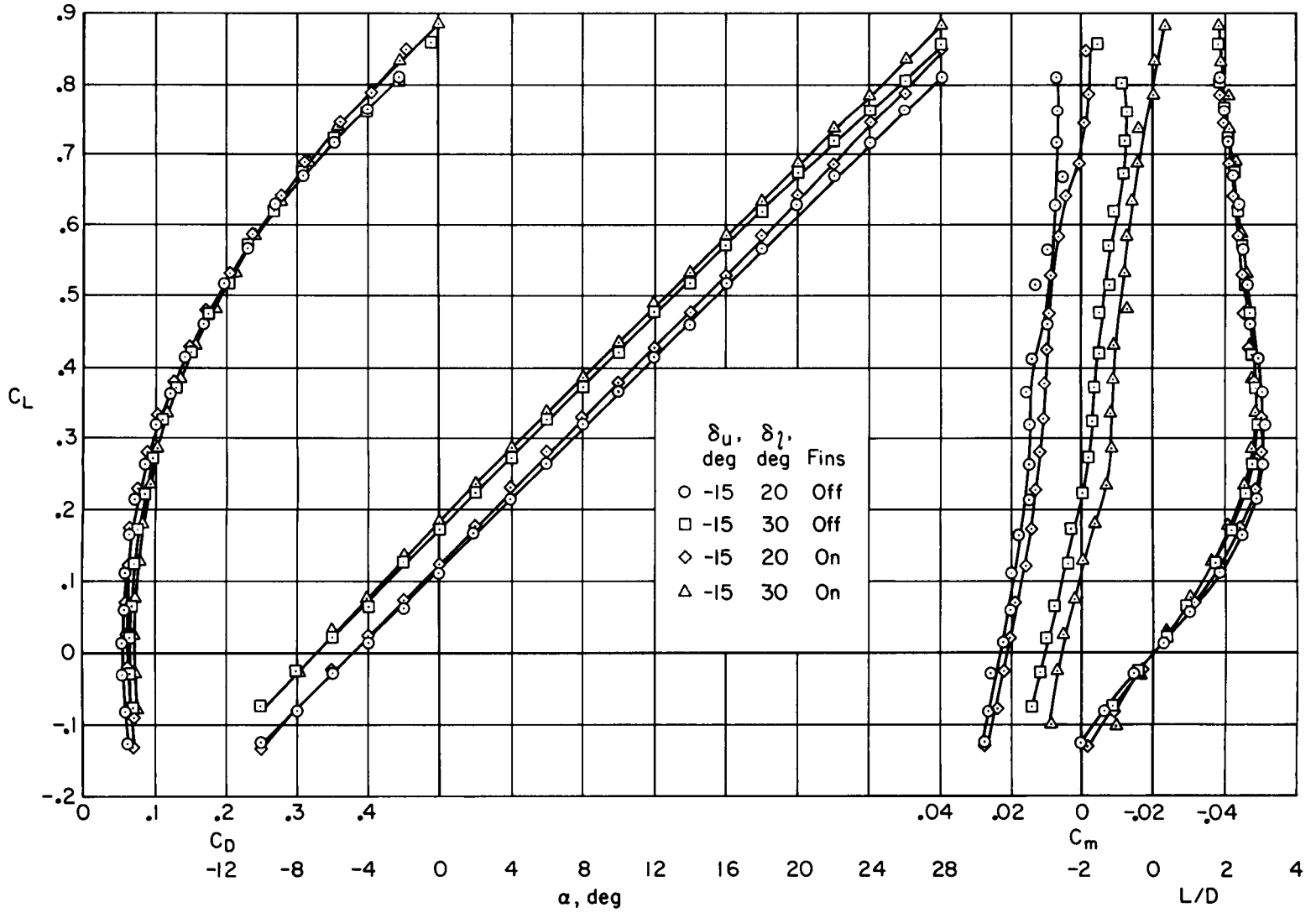

(a) Longitudinal aerodynamic characteristics.

Figure 16.- The effects of the thick outboard ventral fins on the aerodynamic characteristics of the basic M2-F2 configuration.

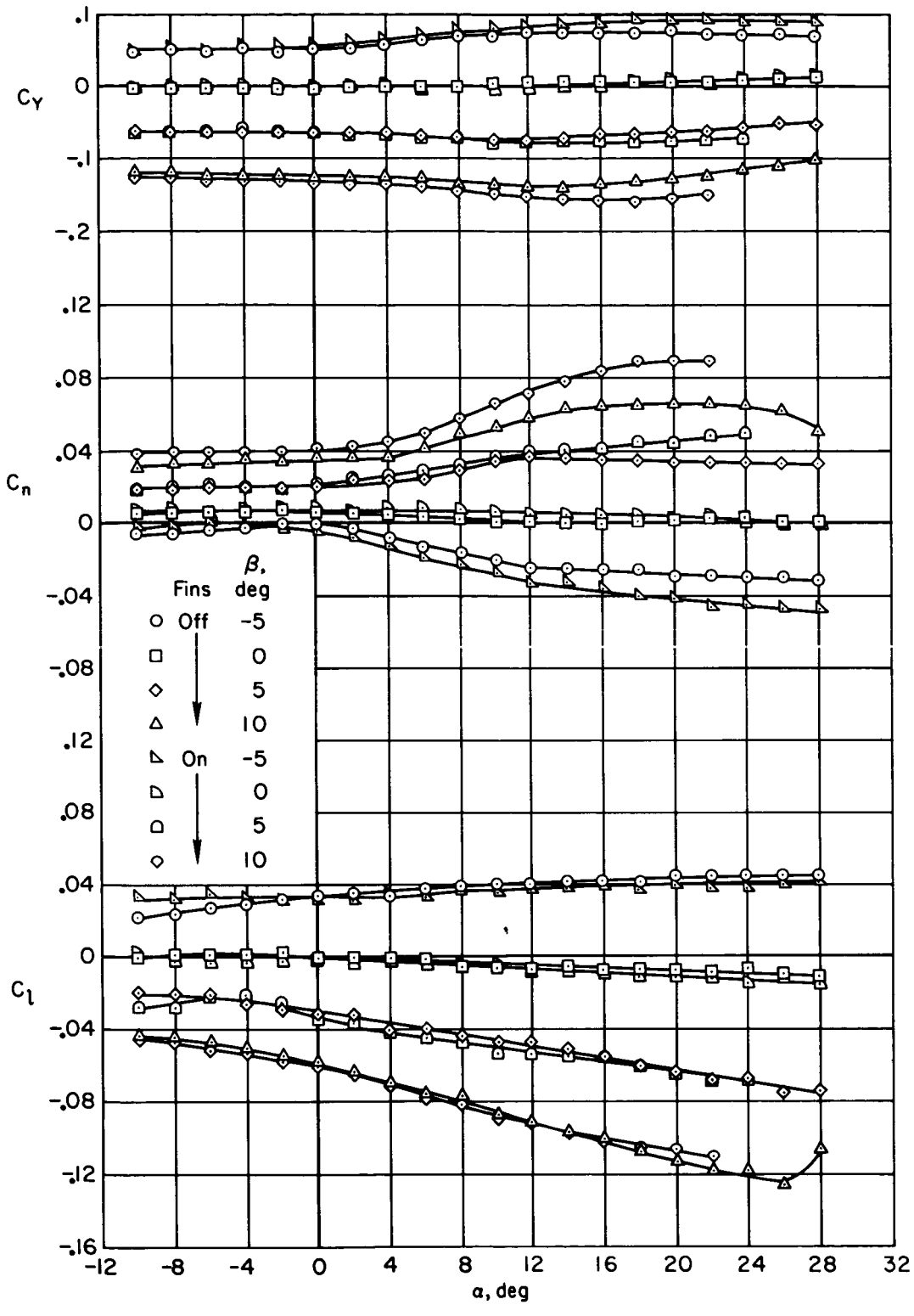

(b) Lateral-directional aerodynamic characteristics; $\delta_u = -15^\circ$, $\delta_l = 30^\circ$.

Figure 16.- Concluded.

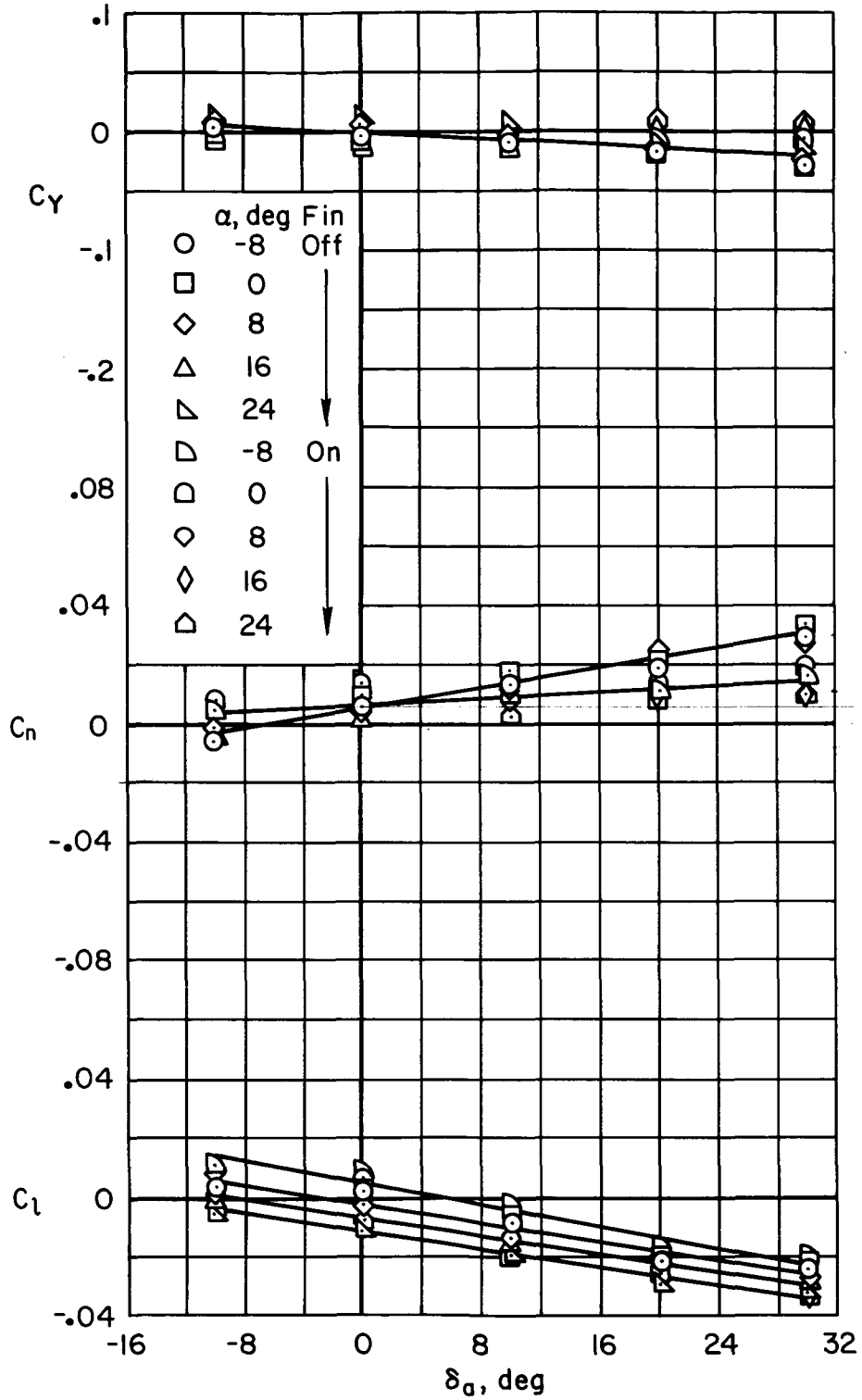

Figure 17.- The effects of the dorsal fin on the lateral control effectiveness of the basic M2-F2 configuration; $\delta_u = -10^\circ$, $\delta_l = 20^\circ$.

~~CONFIDENTIAL~~

UNCLASSIFIED

"The aeronautical and space activities of the United States shall be conducted so as to contribute . . . to the expansion of human knowledge of phenomena in the atmosphere and space. The Administration shall provide for the widest practicable and appropriate dissemination of information concerning its activities and the results thereof."

—NATIONAL AERONAUTICS AND SPACE ACT OF 1958

NASA SCIENTIFIC AND TECHNICAL PUBLICATIONS

TECHNICAL REPORTS: Scientific and technical information considered important, complete, and a lasting contribution to existing knowledge.

TECHNICAL NOTES: Information less broad in scope but nevertheless of importance as a contribution to existing knowledge.

TECHNICAL MEMORANDUMS: Information receiving limited distribution because of preliminary data, security classification, or other reasons.

CONTRACTOR REPORTS: Technical information generated in connection with a NASA contract or grant and released under NASA auspices.

TECHNICAL TRANSLATIONS: Information published in a foreign language considered to merit NASA distribution in English.

TECHNICAL REPRINTS: Information derived from NASA activities and initially published in the form of journal articles.

SPECIAL PUBLICATIONS: Information derived from or of value to NASA activities but not necessarily reporting the results of individual NASA-programmed scientific efforts. Publications include conference proceedings, monographs, data compilations, handbooks, sourcebooks, and special bibliographies.

Details on the availability of these publications may be obtained from:

SCIENTIFIC AND TECHNICAL INFORMATION DIVISION

NATIONAL AERONAUTICS AND SPACE ADMINISTRATION

Washington, D.C. 20546

~~CONFIDENTIAL~~